

Enhanced signal of momentum broadening in hard splittings for γ -tagged jets in a multistage approach

Y. Tachibana,^{1,*} C. Sirimanna,^{2,3} A. Majumder,³ A. Angerami,⁴ R. Arora,⁵ S. A. Bass,² Y. Chen,^{6,7,8} R. Datta,³ L. Du,^{9,10,11} R. Ehlers,^{10,11} H. Elfner,^{12,13,14} R. J. Fries,^{15,16} C. Gale,⁹ Y. He,¹⁷ B. V. Jacak,^{10,11} P. M. Jacobs,^{10,11} S. Jeon,⁹ Y. Ji,¹⁸ F. Jonas,^{10,11} L. Kasper,⁶ M. Kordell II,^{15,16} A. Kumar,^{19,9} R. Kunnawalkam-Elayavalli,⁶ J. Latessa,⁵ Y.-J. Lee,^{7,8} R. Lemmon,²⁰ M. Luzum,²¹ S. Mak,¹⁸ A. Mankolli,⁶ C. Martin,²² H. Mehryar,⁵ T. Mengel,²² C. Nattrass,²² J. Norman,²³ C. Parker,^{15,16} J.-F. Paquet,⁶ J. H. Putschke,³ H. Roch,³ G. Roland,^{7,8} B. Schenke,²⁴ L. Schwiebert,⁵ A. Sengupta,^{15,16} C. Shen,^{3,25} M. Singh,⁶ D. Soeder,² R. A. Soltz,^{3,4} I. Soudi,^{26,27,3} J. Velkovska,⁶ G. Vujanovic,¹⁹ X.-N. Wang,^{28,10,11} X. Wu,^{9,3} and W. Zhao^{10,11,3}
(JETSCAPE Collaboration)

¹*Akita International University, Yuwa, Akita-city 010-1292, Japan.*

²*Department of Physics, Duke University, Durham, North Carolina 27708, USA*

³*Department of Physics and Astronomy, Wayne State University, Detroit, Michigan 48201, USA.*

⁴*Lawrence Livermore National Laboratory, Livermore, California 94550, USA.*

⁵*Department of Computer Science, Wayne State University, Detroit, Michigan 48202, USA.*

⁶*Department of Physics and Astronomy, Vanderbilt University, Nashville, Tennessee 37235, USA.*

⁷*Laboratory for Nuclear Science, Massachusetts Institute of Technology, Cambridge, Massachusetts 02139, USA.*

⁸*Department of Physics, Massachusetts Institute of Technology, Cambridge, Massachusetts 02139, USA.*

⁹*Department of Physics, McGill University, Montréal, Québec H3A 2T8, Canada.*

¹⁰*Department of Physics, University of California, Berkeley, California 94720, USA.*

¹¹*Nuclear Science Division, Lawrence Berkeley National Laboratory, Berkeley, California 94720, USA.*

¹²*GSI Helmholtzzentrum für Schwerionenforschung, 64291 Darmstadt, Germany.*

¹³*Institute for Theoretical Physics, Goethe University, 60438 Frankfurt am Main, Germany.*

¹⁴*Frankfurt Institute for Advanced Studies, 60438 Frankfurt am Main, Germany.*

¹⁵*Cyclotron Institute, Texas A&M University, College Station, Texas 77843, USA.*

¹⁶*Department of Physics and Astronomy, Texas A&M University, College Station, Texas 77843, USA.*

¹⁷*School of Physics and Optoelectronics, South China University of Technology, Guangzhou 510640, China.*

¹⁸*Department of Statistical Science, Duke University, Durham, North Carolina 27708, USA.*

¹⁹*Department of Physics, University of Regina, Regina, Saskatchewan S4S 0A2, Canada.*

²⁰*STFC Daresbury Laboratory, Daresbury, Warrington WA4 4AD, United Kingdom.*

²¹*Instituto de Física, Universidade de São Paulo, C.P. 66318, 05315-970 São Paulo, São Paulo, Brazil.*

²²*Department of Physics and Astronomy, University of Tennessee, Knoxville, Tennessee 37996, USA.*

²³*Oliver Lodge Laboratory, Department of Physics, University of Liverpool, Oxford Street, Liverpool L69 7ZE, United Kingdom.*

²⁴*Department of Physics, Brookhaven National Laboratory, Upton, New York 11973, USA.*

²⁵*RIKEN BNL Research Center, Brookhaven National Laboratory, Upton, New York 11973, USA.*

²⁶*University of Jyväskylä, Department of Physics, P.O. Box 35, FI-40014 University of Jyväskylä, Finland.*

²⁷*Helsinki Institute of Physics, P.O. Box 64, FI-00014 University of Helsinki, Finland.*

²⁸*Key Laboratory of Quark and Lepton Physics (MOE) and Institute of Particle Physics, Central China Normal University, Wuhan 430079, China.*

We investigate medium-induced modifications to jet substructure observables that characterize hard splitting patterns in central Pb-Pb collisions at the top energy of the Large Hadron Collider (LHC). Using a multistage Monte Carlo simulation of in-medium jet shower evolution, we explore flavor-dependent medium effects through simulations of inclusive and γ -tagged jets. The results show that quark jets undergo a non-monotonic modification compared to gluon jets in observables such as the Pb-Pb to p - p ratio of the Soft Drop prong angle r_g , the relative prong transverse momentum $k_{T,g}$ and the groomed mass m_g distributions. Due to this non-monotonic modification, γ -tagged jets, enriched in quark jets, provide surprisingly clear signals of medium-induced structural modifications, distinct from effects dominated by selection bias. This work highlights the potential of hard substructures in γ -tagged jets as powerful tools for probing the jet-medium interactions in high-energy heavy-ion collisions. All simulations for γ -tagged jet analyses carried out in this paper used triggered events containing at least one hard photon, which highlights the utility of these observables for future Bayesian analysis.

I. INTRODUCTION

High-energy heavy-ion collision experiments at the Relativistic Heavy Ion Collider (RHIC) and the Large Hadron Collider (LHC) have established jets as essen-

* Contact author: ytachibana@aiu.ac.jp

tial tools to probe the quark-gluon plasma (QGP), a strongly coupled, deconfined state of matter created in these collisions [1–20]. Large transverse momentum partons generated in the initial hard scatterings traverse the QGP medium, undergoing significant interactions that lead to observable modifications compared to proton-proton (p - p) collisions, where a sufficiently large medium is not formed [21]. Early measurements at RHIC, such as the suppression of high transverse momentum hadrons [22–26] and the disappearance of di-hadron correlations [27–29], provided the first experimental evidence of parton energy loss due to the strong interactions with the QGP medium. Recent advances at RHIC and LHC have allowed more detailed studies of reconstructed jets [30–33], providing deeper insights into the fundamental mechanisms underlying jet-medium interactions, such as medium-induced radiation, scattering with medium constituents, in-medium thermalization, the hydrodynamic evolution of energy deposited by jets, etc.

The loss of jet transverse momentum (p_T^{jet}), as revealed by the nuclear modification factor R_{AA} , has been a central focus of measurements and analyses, establishing R_{AA} as a primary observable. However, the extent of p_T^{jet} loss in reconstructed jets depends only on the energy and momentum that has been scattered or radiated outside the jet cone. Partons in hard showers lose energy by scattering and radiation. The extra scattering in the medium changes not only the energy radiated outside the cone but also the energy-momentum distribution within the cone. The latter can only be accessed via jet substructure observables. Investigating jet substructures also necessitates triggering on jets based on their p_T^{jet} , making an accurate calculation of p_T^{jet} loss essential. To explore jet-medium interactions effectively, it is crucial to study both the p_T^{jet} loss, reflected in the R_{AA} , and the internal structure modifications, captured by substructure observables.

Recent years have seen a proliferation of observables and analysis techniques referred to as jet substructure, with examples including the jet fragmentation function, jet mass, and jet shape. These reveal medium effects on the internal structure of jets [30–57]. Advanced grooming techniques [58–64] extract imprints of hard partonic branchings—occurring early in jet evolution—from final-state hadrons forming reconstructed jets, even though such branchings cannot be directly observed experimentally. Understanding these hard branchings, which form the skeleton of a jet’s internal structure, is crucial to uncovering how jet structures are shaped and modified by medium effects, ultimately leading to p_T^{jet} loss. In vacuum, hard branchings are relatively well-described using perturbative methods, offering robust baselines for studying medium-induced modifications in heavy-ion collisions. Hard branchings have also attracted significant theoretical interest, as they provide a promising avenue to explore jet-medium interactions [64–75].

Soft Drop [62], one of the most widely used grooming methods in heavy-ion physics, identifies two hard prongs

with the largest angular separation within the jet while discarding low-momentum prongs, defining the split as the hardest branching. In our previous study [74], we analyzed the Soft Drop observables z_g (momentum fraction) and r_g (radial separation) for inclusive jets triggered by their p_T^{jet} , using Monte Carlo simulations of in-medium jet shower evolution with the MATTER+LBT multistage model [20, 76–82] within the JETSCAPE framework [21, 74, 83–93]. The z_g distribution showed negligible medium-induced modifications, consistent with experiments, while the r_g distribution exhibited suppression that increases monotonically with r_g . This monotonic behavior was reproduced by incorporating modified coherence effects [89, 94, 95], where high-virtuality partons, due to finer resolution, perceive the medium as dilute and experience reduced interactions. As a result, jets with larger r_g were strongly suppressed, with no trace of medium-induced broadening in the hard partonic branchings.

These findings suggest that the suppression of the r_g distribution may arise primarily from selection bias in inclusive jet analyses, rather than direct modifications to hard branching structures: Jets with large-angle hard branchings are more likely to lose soft constituents outside the jet cone, leading to a preference for triggering on jets with smaller angular separations and reduced energy loss. Thus, inclusive jet measurements are less sensitive to medium-induced changes in hard branching structures, underscoring the need for targeted observables to probe these effects.

To investigate medium-induced modifications to hard branchings in detail, mitigating the selection bias inherent in inclusive jet analyses is essential. This can be achieved using γ -tagged or Z -tagged jets, produced in photon-jet or Z -boson-jet pair production events, often referred to as *golden channels*. Photons and Z bosons do not interact strongly with the QGP medium. Thus, photons and Z bosons that are pair-produced with a jet in the initial hard scattering are measured with transverse momenta (p_T) that closely approximate the initial p_T of the partons generating the jets, at leading order. Triggering on the p_T of the photon or Z boson, instead of the jet, selects jets with similar initial p_T , independent of p_T^{jet} loss, reducing selection bias and enabling cleaner investigations of medium effects on jet structures. Additionally, partons paired with photons or Z bosons are predominantly quarks, minimizing flavor-dependent selection bias. Comparing these tagged jets with inclusive jets allows systematic studies of flavor-dependent effects.

In this paper, we investigate γ -tagged jets as a means to mitigate the selection bias effect, enabling a clearer examination of medium modifications to a subset of Soft Drop observables that characterize the hard substructure of jets. Building on our previous work [74, 89, 90], which established a wealth of benchmark results, we employ the MATTER+LBT multistage model within the JETSCAPE framework to provide predictions under realistic high-energy heavy-ion collision configurations. We demon-

strate that fixing the photon p_T and triggering on associated jets, even those with lower p_T^{jet} , eliminates the suppression of jets with broad hard splittings observed in inclusive jet measurements. This confirms that the suppression in inclusive jets arises from selection bias rather than intrinsic modifications to the hard-splitting structure. Moreover, we show that γ -tagged jets exhibit pronounced broadening of splittings compared to inclusive jets, driven by their quark-jet dominance. With simplified simulations, we reveal that quark jets are more susceptible to medium-induced modifications, particularly during low-virtuality evolution, leading to significant modifications in their hard branching structure. These results establish γ -tagged jets, and similarly Z -tagged jets, as powerful tools for revealing clear signals of medium modifications to the hard branchings in jets through their substructure observables.

The paper is organized as follows. Section II outlines the simulation framework and methodologies employed, including the multistage MATTER+LBT model within the JETSCAPE framework. In Sec. III, we detail the analysis procedures for γ -tagged jets as well as inclusive jets, including Soft Drop grooming. Section IV presents the results from the JETSCAPE simulations, highlighting the flavor-dependent medium effects and selection biases on r_g , $k_{T,g}$, and m_g distributions, as well as the role of γ -tagged jets in revealing intrinsic medium modifications. Subsequently, in Sec. V, we compare the results from the same event sets with available experimental data from Pb-Pb collisions at the LHC. Finally, Sec. VI concludes with a summary of our findings.

II. MODEL

In this paper, the JETSCAPE code package is utilized, which offers a flexible framework for modular integration in Monte Carlo event generation for heavy-ion collisions. We specifically employ our current default configuration with the MATTER+LBT setup referred to as the JETSCAPEv3.5 AA22 tune, as detailed in our previous work [74, 89, 90], to perform simulations of jet events. All parameters in the tune are chosen to fit only the R_{AA} s for single high- p_T particles and reconstructed jets in Ref. [89] and are not retuned for any other observables, including all the observables presented in this paper. In this section, we provide a brief overview of the components that constitute our simulation setup. For readers interested in delving deeper into the specific physical elements integrated into the multistage MATTER+LBT simulation within the JETSCAPE framework, we direct them to Refs. [74, 89, 90]. Additional insights into the software components of the JETSCAPE framework are detailed in Ref. [83]. The foundational concept concerning the multistage description of jet evolution within the medium is explained in Ref. [82].

A. Overview

For the efficient generation of jet events, the JETSCAPE framework provides an option to embed a single hard scattering event from a nucleon-nucleon collision into a heavy-ion collision event using a pre-generated space-time background profile of the QGP medium.

In the JETSCAPEv3.5 AA22 tune, we employ the background medium profile obtained from event-by-event calculations of $(2+1)$ -dimensional $[(2+1)\text{-D}]$ free-streaming pre-equilibrium evolution [96], followed by viscous hydrodynamic evolution using $(2+1)\text{-D}$ VISHNU [97] and hadronic scattering and decay simulated by URQMD [98, 99], with fluctuating initial conditions from TRENTO [100]. Here the best-fit parametrization, determined through maximum a posteriori (MAP) from Bayesian methods [101] applied to observables measured at the LHC, is used. In jet simulations, high-energy partons are generated according to the hard process settings described later in Subsection II B, and then these partons evolve into parton showers. In the multistage setup of MATTER+LBT, these partons are initially subjected to virtuality-ordered splitting while incorporating medium effects in the MATTER module [76, 77]. The partons then undergo successive parton splittings, rapidly reducing their virtuality. The description of the splittings for a parton in the MATTER module is terminated when its virtuality becomes sufficiently small, approximately on par with the accumulated transverse momentum gain via scatterings in the medium. This termination is attributed to the applicable limit of a model that relies on virtuality as the primary mechanism for branching. The partons with reduced virtuality are then transferred to the LBT module [78, 79, 102], which simulates elastic and inelastic scatterings with medium constituents based on kinetic theory with the on-shell approximation.

In the JETSCAPE framework, this virtuality-based switching between the MATTER and LBT modules is performed bidirectionally at a parton-by-parton level using a switching parameter denoted as Q_{sw}^2 . If the parton's virtuality $Q^2 = p^\mu p_\mu - m^2$ drops below Q_{sw}^2 , it is transferred from MATTER to LBT, and it returns to MATTER when the virtuality exceeds Q_{sw}^2 again or when it exits the QGP medium boundary at a temperature $T_c = 0.16$ GeV. Below T_c , MATTER performs vacuum-like splitting down to the cutoff scale $Q_{\text{min}}^2 = 1$ GeV² without any medium effects. Throughout this study, the switching parameter is set to $Q_{\text{sw}}^2 = 4$ GeV² ($Q_{\text{sw}} = 2$ GeV).

In both the MATTER and LBT phases, the medium effects are calculated based on the local temperature and flow velocity from the pre-generated background medium profile. The medium response is described by following the subsequent evolution of recoil partons scattered out from the medium during the in-medium collisions simulated in MATTER and LBT in the same way as the other showering partons. The recoil partons are assumed to be on-shell at their generation and are then passed to LBT for the following elastic and inelastic processes within the

medium. On the other hand, for each in-medium collision event that generates a recoil parton, a deficit of energy and momentum is left in the medium. This deficit is also tracked and treated as a freestreaming particle, referred to as a hole parton.

All jet partons undergo hadronization via the COLORLESS HADRONIZATION module, in which the Lund string model of PYTHIA 8 is utilized after escaping the QGP medium with $T > T_c$ and reaching the virtuality cutoff scale Q_{\min}^2 . The jet shower partons, including the recoils and further accompanying daughters, are collectively hadronized, whereas the hole partons are hadronized separately. Using those hadrons formed by clustering hole partons, appropriate subtraction is performed depending on the observable of interest. In this study, the hole hadrons are tagged for identification and, together with the other hadrons, sent to a modified anti- k_t jet reconstruction routine, in which the four-momentum of hole hadrons or reconstructed subjets dominated by hole hadrons is subtracted during the merging process in the E -scheme [103].

Incidentally, in the later stages of in-medium jet evolution, as a jet parton energy becomes close to the scale of the ambient temperature, the approach based on kinetic theory becomes less practical due to the short mean free paths. Such soft components of jets are expected to be thermalized and then transported hydrodynamically through the bulk medium flow [19, 104–109]. The hydrodynamic description of the evolution of the soft components of jets, as proposed in Refs. [110–131], can be implemented, through a source term, by coupling with the hydrodynamic equation for the bulk evolution. However, this approach necessitates a comprehensive (3 + 1)-D hydrodynamic simulation for each jet event and makes the computational cost of conducting a systematic and exhaustive study, as demonstrated in this paper, outstandingly expensive. Therefore, this paper primarily focuses on the hard part of the jets, deferring a detailed study of the effects of the soft components to future research.

Calculations for p - p collisions are also necessary to establish a baseline for the heavy-ion collision simulations. Our p - p calculations are also performed using the JETSCAPE framework, with all medium effects turned off, where the parton shower evolution is managed solely by MATTER without jet-medium coupling. This configuration is known as the JETSCAPE PP19 tune and is described in detail in Ref. [84].

B. Initial hard process

In this paper, we compare our results from the JETSCAPE simulations with several different settings for the initial hard process generation. Below, we explain each setting. With any setting, the geometric position in the transverse plane at mid-space-time rapidity ($\eta_s = (1/2) \ln[(t+z)/(t-z)] = 0$), where the hard process occurs is determined by sampling the N_{coll} distribution

calculated using the TRENTO initial condition module for the Pb-Pb collisions.

1. *PGun*

To serve as a test for systematic studies with minimal extraneous contributions and simplified settings, we generate events with just a single high-energy parton and simulate its jet shower development. Within the JETSCAPE package, such a setup is enabled by the PGUN module. In PGUN, one specifies the species of the parton and its initial energy and then shoots it onto the transverse plane at mid-space-time rapidity ($\eta_s = 0$) with a randomly assigned azimuthal direction. The generated partons are then passed to a module handling high-virtuality parton development, MATTER in this study, initiating the jet shower. In this study, we compare scenarios with either a gluon or a massless light quark as the initial parent parton.

2. *PythiaGun*

For the generation of realistic jet events in hadron-hadron collisions, the JETSCAPE framework provides the PYTHIAGUN module, which serves as a wrapper for PYTHIA 8 [132]. Within the PYTHIAGUN module, utilizing the functionalities of PYTHIA 8, hard scatterings are generated based on leading-order perturbation calculations. Subsequently, final state radiation (FSR) is disabled by default, and the resulting hard partons are directly passed to a module responsible for the evolution of highly virtual partons, MATTER in this study, to facilitate the development of jet showers. Simultaneously, when initial state radiation (ISR) or multiparton interaction (MPI) is turned on, the partons produced through such a process are also passed to the jet shower evolution. Throughout this study, both ISR and MPI are always on for initial scattering generation using PYTHIAGUN.

Hard γ -jet pair production is a very rare process. In a fully inclusive event generation scheme, most events are not triggered, making it extremely challenging to accumulate sufficient statistics for the differential observables of jet substructure, which are the focus of this study. To address this, we adopt a strategy that selectively generates only the initial hard processes with leading-order contributions involving prompt-photon production, by configuring PYTHIAGUN with `HardQCD:all=off` and `PromptPhoton:all=on`, thereby enhancing computational efficiency. While this method does not fully account for the contribution from jet-photon production via fragmented photons, our main predictions focus on the region where these effects are minimal ($x_{J\gamma} < 1$, i.e., $p_T^\gamma > p_T^{\text{jet}}$), as demonstrated in our previous study [93]. In contrast, for the inclusive jet analysis, we generate events by enabling all hard QCD 2-to-2 processes through the settings `HardQCD:all=on`.

In the actual experimental analysis, the isolation cut mentioned later in Subsec. III B is applied to select γ -tagged jets to enhance the leading-order contributions in initial hard scatterings involving prompt photon production. However, in practice, perfect extraction is not achievable, and contributions beyond leading-order prompt photons unavoidably seep in. For example, if a photon is emitted at a large angle from a parton jet shower, it may pass the isolation cut requirement.

Further discussions concerning the evaluation of the contributions of photons radiated from parton showers to the γ -tagged jet can be found in our separate study [93]. Additionally, the behaviors observed in the γ -tagged jet results presented in this paper are also expected to appear in Z -tagged jet measurements, as both are boson-tagged observables that offer similar advantages: cleaner access to the initial parton kinematics and strong quark-jet dominance. Due to their large masses, Z -boson radiations from parton showers are drastically suppressed, making those produced at leading order in the initial hard scatterings completely dominant in measurements.

III. ANALYSES

This section provides a detailed description of the Soft Drop grooming procedure used for calculating observables that characterize the hard component structures of jets, as well as the method for constructing γ -tagged jets in our Monte Carlo simulations of high-energy heavy-ion collisions.

A. Soft Drop grooming procedure

In this study, we focus on observables characterizing hard splittings of jets obtained through the Soft Drop grooming algorithm [62]. The Soft Drop grooming identifies the hard splitting, while removing the soft branchings, at as large an angle as possible.

In the Soft Drop grooming procedure, an angular-ordered clustering tree is rebuilt using the Cambridge-Aachen (C/A) algorithm [133, 134] for constituents of a triggered jet reconstructed by a standard jet-finding algorithm, such as the anti- k_t algorithm [135], with a jet cone size R . Next, we traverse back, i.e., from the branch with the largest angle, through the C/A tree. At each branching, we check whether the two prongs of the branching satisfy the Soft Drop condition given by

$$\frac{p_{T,1}, p_{T,2}}{p_{T,1} + p_{T,2}} > z_{\text{cut}} \left(\frac{\Delta R_{12}}{R} \right)^\beta, \quad (1)$$

where $p_{T,1}$ and $p_{T,2}$ ($< p_{T,1}$) are the transverse momenta of the prongs, and $\Delta R_{12} = \sqrt{(\eta_1 - \eta_2)^2 + (\phi_1 - \phi_2)^2}$ is the radial distance between the prongs in the rapidity-azimuthal angle plane. The Soft Drop parameters z_{cut} and β control the grooming procedure.

If the Soft Drop condition is satisfied, we stop the procedure, and the two prongs of the branching are used to calculate the groomed jet observables. If the condition is not met, we continue traversing the tree by following the prong with the larger p_T and repeat the same procedure. It should be noted that there may be cases where a prong pair satisfying the Soft Drop condition cannot be found eventually. Throughout this work, the jet reconstruction and Soft Drop grooming are performed using the FASTJET package [136, 137] with FASTJET-CONTRIB-1.045 [138].

B. γ -tagged jet

Photons do not interact strongly with the QGP medium. This characteristic is particularly notable in the leading-order contribution to γ -jet pair production in the initial hard scattering in high-energy heavy-ion collisions. The photons produced in such events are typically measured with transverse momentum nearly identical to the initial transverse momentum of the jet's parent parton. This correlation enables the estimation of the jet's energy loss due to medium interactions.

However, experimentally, γ -jet pairs can also arise from processes other than the initial hard γ -jet pair creation, such as photon radiation in final state parton showering. Therefore, to suppress contamination from such non-targeted processes, specific cuts are imposed in the experimental analyses: the isolation requirement for photons and the relative azimuth angle cut. To enhance quantitative accuracy in our comparison to experimental data, we impose these cuts on our simulated events.

The isolation requirement, specifically the selection of photons with minimal energy emissions in their vicinity, is introduced to enhance the leading-order contributions. Photons are isolated based on the accumulated transverse energy or momentum inside a cone of fixed radius of size R_{iso} centered on the photon's direction after subtracting background contributions. In this study, they are calculated as follows:

$$E_T^{\text{iso}} = \left(\sum_{\substack{i \in \text{shower} \\ \Delta r_i < R_{\text{iso}}}} E_{T,i} \right) - \left(\sum_{\substack{i \in \text{holes} \\ \Delta r_i < R_{\text{iso}}}} E_{T,i} \right) - E_T^\gamma, \quad (2)$$

$$p_T^{\text{iso}} = \left(\sum_{\substack{i \in \text{shower} \\ \Delta r_i < R_{\text{iso}}}} p_{T,i} \right) - \left(\sum_{\substack{i \in \text{holes} \\ \Delta r_i < R_{\text{iso}}}} p_{T,i} \right) - p_T^\gamma, \quad (3)$$

where $\Delta r_i = [(\eta_i - \eta_\gamma)^2 + (\phi_i - \phi_\gamma)^2]^{1/2}$ is the radial distance from the isolated photon candidate. On the right-hand sides, the sums are taken over final-state particles from hadronization of jet shower partons, including the recoils in the first terms and over particles hadronized from hole partons in the second terms, respectively. The transverse energy and momentum of the isolated photon candidate in the last terms are introduced to eliminate self-contribution. If the candidate satisfies either

$E_T^{\text{iso}} < E_T^{\text{iso,cut}}$ or $p_T^{\text{iso}} < p_T^{\text{iso,cut}}$, based on the pre-determined cut parameter $E_T^{\text{iso,cut}}$ or $p_T^{\text{iso,cut}}$, depending on the analysis method used in the experimental results for comparison, it qualifies as an isolated photon.

The relative azimuth angle cut,

$$|\phi_{\text{jet}} - \phi_\gamma| > \Delta\phi_{\text{cut}}, \quad (4)$$

is introduced to ensure that the photon and jet are back-to-back in the azimuthal angle plane, thereby enhancing the leading-order contribution from the initial hard γ -jet pair production. The cut value most commonly used in various experiments is $\Delta\phi_{\text{cut}} = 7\pi/8$.

IV. RESULTS

This section systematically investigates the modification of the Soft Drop substructures from simulations with simplified initial events generated by the PGUN module. A single quark or gluon is generated at one point in the medium and allowed to propagate outward. Strict control over the flavor and energy of the parton allows for a detailed investigation of the flavor and energy dependence of specific substructure observables.

Following this, we present theoretical predictions for γ -tagged jets using realistic initial events generated by PYTHIAGUN. These are compared with the results from inclusive jets, and novel, experimentally measurable signals of medium effects in these observables are discussed. To establish the reliability of the model calculations and provide a baseline for discussion, comparisons with available experimental results are presented in the subsequent section, Sec. V.

A. Jet splitting momentum fraction

We begin with the study of the medium modification of the jet splitting momentum fraction z_g , which is defined as

$$z_g = \frac{p_{T,2}}{p_{T,1} + p_{T,2}}, \quad (5)$$

where $p_{T,1}$ and $p_{T,2}$ ($< p_{T,1}$) are transverse momenta of the pair prongs passing the Soft Drop condition.

In Fig. 1, the results for leading jets from PGUN simulations for the vacuum case are shown. The initial energy of the parent parton is fixed at $E_{\text{init}} = 140$ GeV. In the upper panel, the z_g distribution normalized by the number of all triggered jets, including those that did not pass the Soft Drop condition,

$$\frac{1}{N_{\text{jet}}} \frac{dN_{\text{SD,jet}}}{dz_g}, \quad (6)$$

is shown, whereas in the lower panel, the one normalized by the number of jets passing the Soft Drop condition,

$$\frac{1}{N_{\text{SD,jet}}} \frac{dN_{\text{SD,jet}}}{dz_g}, \quad (7)$$

is shown. Here, N_{jet} and $N_{\text{SD,jet}}$ are the number of triggered jets and the number of jets passing the Soft Drop condition, respectively.

Gluon jets pass the Soft Drop condition more often than quark jets, and as a result, for the case of the normalization by the number of all triggered jets, the gluon jet consistently exhibits larger values than the quark jet across the entire z_g region. However, when normalized by the number of jets passing the Soft Drop condition, the difference between quark jets and gluon jets is nearly negligible.

Figure 2 shows the modification of the z_g distribution for jets generated by PGUN as they pass through the medium created in central (0%–10%) Pb-Pb collisions at $\sqrt{s_{NN}} = 5.02$ TeV. For both quark jets and gluon jets, the modification pattern of a slight shift from small to large z_g behavior is observed without any clear dependence on the value of the p_T^{jet} trigger. Thus, there is no modification attributed to the bias, solely due to energy loss, in the z_g distribution, at least when considering quark jets and gluon jets separately.

Next, we delve into the detailed exploration of how the medium effects at high virtuality and low virtuality, respectively, bring about the hard splitting modification. To achieve this, we conduct simulations incorporating only the medium effects of MATTER, by turning off the medium effects at low virtuality ($Q < 2$ GeV), and present the results of these simulations with the PGUN initial hard process in Fig. 3. For both quark jets and gluon jets, the modification in the z_g distribution is almost invisible, indicating that the modifications observed in the full MATTER+LBT results are governed by the low-virtuality phase, as modeled by the LBT module.

Finally, we examine jets in more realistic events involving hard scattering in p - p collisions at $\sqrt{s} = 5.02$ TeV, generated using the PYTHIAGUN module. The results for γ -tagged jets and inclusive jets with the same p_T^{jet} triggers are compared in Fig. 4. For the γ -tagged jet analysis, only events including prompt photon production at leading order in the initial hard processes are selectively generated with the PYTHIA option `HardQCD:all=off` along with `PromptPhoton:all=on`.

The analysis of γ -tagged jets involves first identifying the leading photon with the highest p_T in each event that satisfies the trigger conditions. All jets associated with this leading photon and meeting the trigger criteria are then counted. To mimic the realistic experimental analysis, the isolation requirement $E_T^{\text{iso}} < 5$ GeV and the relative azimuth angle cut $|\phi_{\text{jet}} - \phi_\gamma| < 7\pi/8$ are imposed. To further suppress the unwanted contribution from photon radiation from jets, we employ the additional cut of $p_T^{\text{jet}} < p_T^\gamma$.

For the inclusive jet analysis, events with initial scatterings, including all hard QCD 2-to-2 events (`HardQCD:all=on+PromptPhoton:all=on`) are used. In the distributions normalized by the number of all triggered jets (upper panel), it can be observed that inclusive jets are slightly more likely to pass the Soft Drop

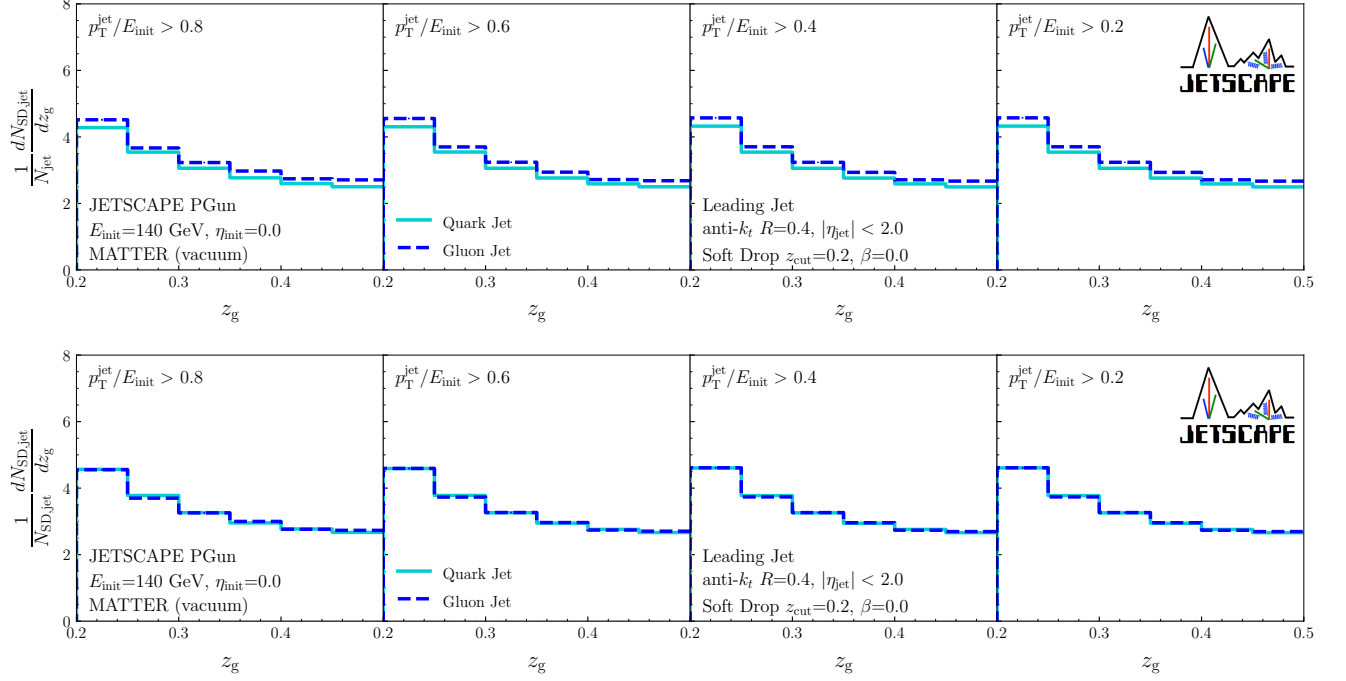


FIG. 1. Distributions of jet splitting momentum fraction z_g normalized by the number of all triggered jets (upper panel) and the number of jets passing the Soft Drop condition (lower panel) for the leading jets in events generated with PGUN. The jet shower evolution is performed by vacuum MATTER for the parent parton having a $E_{\text{init}} = 140$ GeV. Jets are reconstructed with $R = 0.4$ at midrapidity $|\eta_{\text{jet}}| < 2.0$. The results are shown for quark jets (solid) and gluon jets (dashed) with different p_T^{jet} triggers, 112, 84, 56, and 28 GeV. The Soft Drop parameters are $z_{\text{cut}} = 0.2$ and $\beta = 0$.

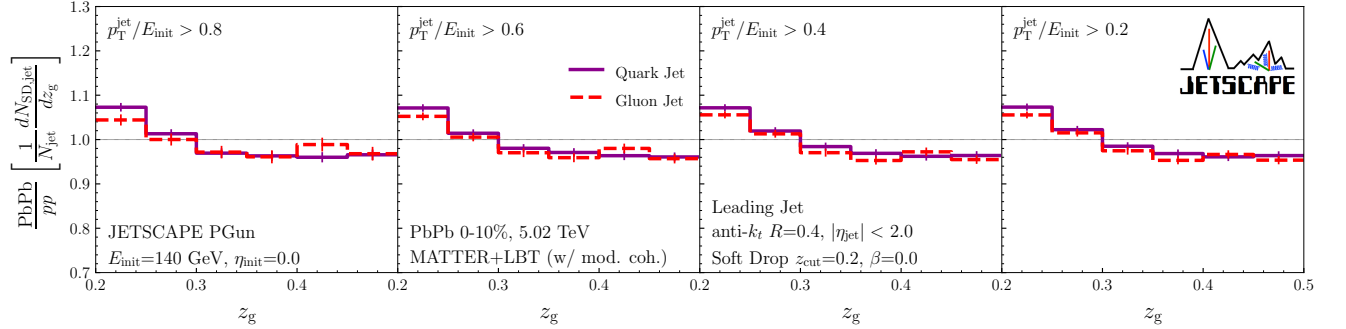


FIG. 2. Ratios of z_g distributions for the leading jets in events with the parent parton having a fixed initial energy $E_{\text{init}} = 140$ GeV generated by PGUN. The jet shower evolution in the QGP medium produced in 0%–10% Pb-Pb collisions at $\sqrt{s_{NN}} = 5.02$ TeV is performed by MATTER+LBT. The results are shown for quark jets (solid) and gluon jets (dashed) with different p_T^{jet} triggers, 112, 84, 56, and 28 GeV. The Soft Drop parameters are $z_{\text{cut}} = 0.2$ and $\beta = 0$.

condition compared to γ -triggered jets, due to the larger fraction of gluon jets. When the normalization is done by the number of jets passing the Soft Drop condition, the difference between γ -triggered jets and inclusive jets disappear, similar to the erasing of differences between gluon and quark jets as seen in the PGUN results.

Figure 5 shows the medium modification for the γ -tagged and inclusive jets in Pb-Pb collisions at $\sqrt{s_{NN}} = 5.02$ TeV with the same triggers. For both γ -tagged jets and inclusive jets, modification becomes less significant

as p_T^{jet} increases. Especially for jets with $p_T^{\text{jet}} > 300$ GeV, almost no changes in the shape of the z_g distribution are observed. In all z_g regions, jets passing the Soft Drop condition are almost uniformly reduced due to medium effects, with the reduction being slightly more pronounced for inclusive jets.

Figure 6 shows our prediction for the $x_{J\gamma}$ dependence in the modification of z_g distribution for γ -tagged jets in Pb-Pb collisions at $\sqrt{s_{NN}} = 5.02$ TeV. As seen in the PGUN results, there is no significant p_T^{jet} -selection bias ef-

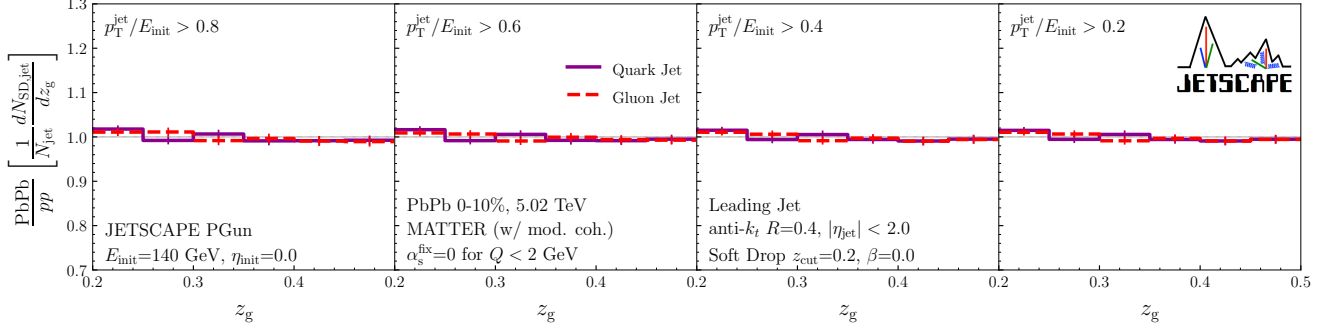


FIG. 3. Same as Fig. 2 for MATTER alone simulations, where the medium effect is turned off for jet partons with virtuality $Q < 2$ GeV.

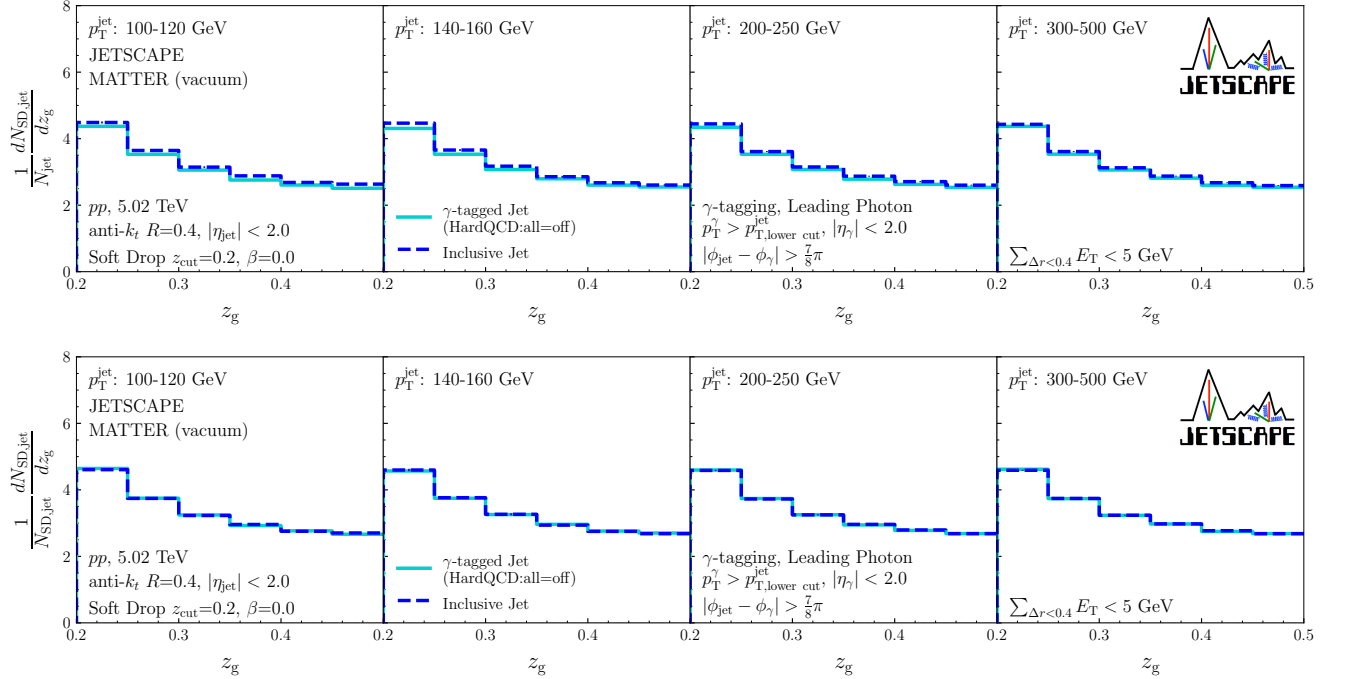


FIG. 4. Same as Fig. 1 for jets from hard scatterings in p - p collisions at $\sqrt{s} = 5.02$ TeV, generated by PYTHIAGUN with ISR and MPI. The results are shown for γ -tagged jets (solid) from prompt photon-generating hard processes (`HardQCD:all=off+PromptPhoton:all=on`) and inclusive jets (dashed) from inclusive hard processes (`HardQCD:all=on+PromptPhoton:all=on`) generated at leading order by PYTHIA 8 and with different p_T^{jet} triggers. For γ -tagged jets, isolation requirement, relative azimuth angle cut, and the additional cut of $p_T^{\text{jet}} < p_T^{\gamma}$ are imposed.

fect on the z_g distribution, and thus, the modification remains almost consistent across all presented $x_{J\gamma}$ ranges.

B. Jet splitting radius

Next, we investigate the medium modification of the jet splitting radius r_g , which is defined as

$$r_g = \sqrt{(\eta_1 - \eta_2)^2 + (\phi_1 - \phi_2)^2}, \quad (8)$$

where η_1 , η_2 , ϕ_1 , and ϕ_2 are the rapidities and azimuthal angles of the pair prongs passing the Soft Drop condition.

In Fig. 7, the r_g distributions normalized by N_{jet} ,

$$\frac{1}{N_{\text{jet}}} \frac{dN_{\text{SD},\text{jet}}}{dr_g}, \quad (9)$$

for leading gluon jets and quark jets from the vacuum PGUN simulations are compared. The gluon jets exhibit much wider distributions with a peak at larger r_g values than quark jets. This is due to the fact that gluon jets, having a larger Casimir factor and radiating more, tend to be produced with a larger virtuality compared to

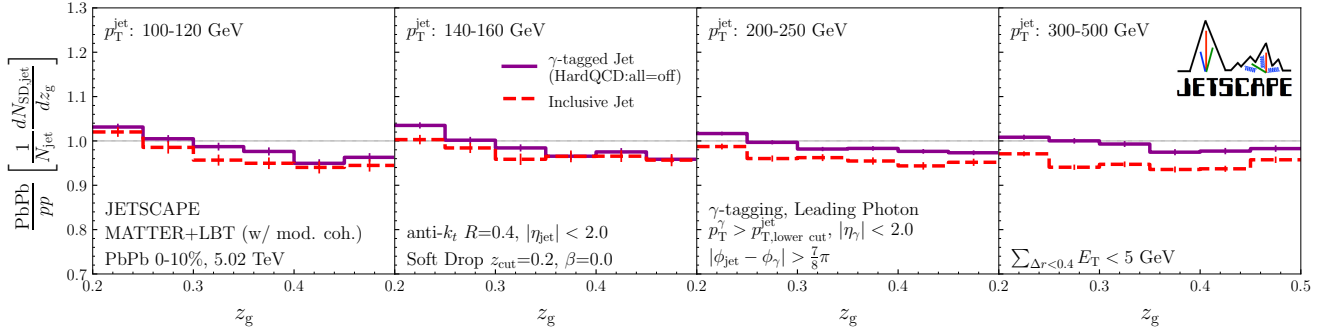


FIG. 5. Same as Fig. 2 for jets from hard scatterings at $\sqrt{s_{NN}} = 5.02$ TeV, generated by PYTHIA-GUN with ISR and MPI. The results are shown for γ -tagged jets (solid) from prompt photon-generating hard processes (`HardQCD:all=off+PromptPhoton:all=on`) and inclusive jets (dashed) from inclusive hard processes (`HardQCD:all=on+PromptPhoton:all=on`) generated at leading order by PYTHIA 8 with different p_T^{jet} triggers. For γ -tagged jets, isolation requirement, relative azimuth angle cut, and the additional cut of $p_T^{\text{jet}} < p_T^{\gamma}$ are imposed.

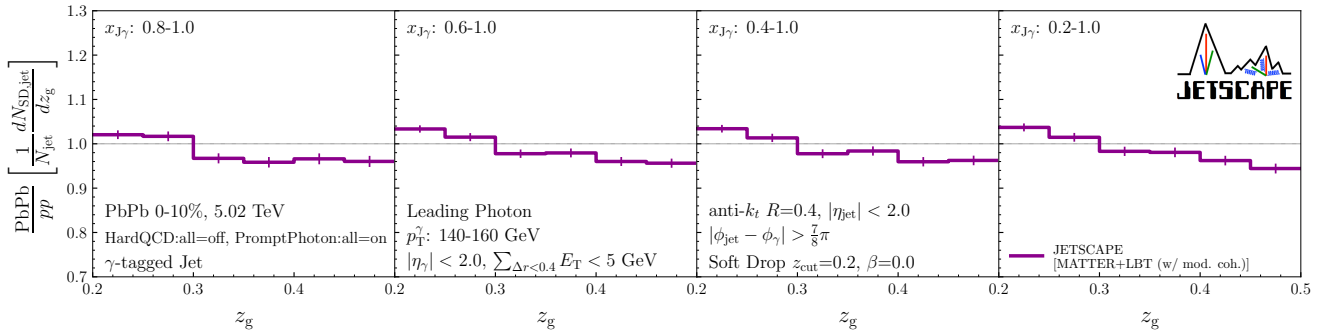


FIG. 6. Same as Fig. 2 for γ -tagged jets from prompt photon-generating hard processes (`HardQCD:all=off+PromptPhoton:all=on`) generated at leading order by PYTHIA 8 at $\sqrt{s_{NN}} = 5.02$ TeV for different x_{J_γ} ranges. The photon of $140 < p_T^{\gamma} < 160$ GeV is triggered with isolation requirement, relative azimuth angle cut.

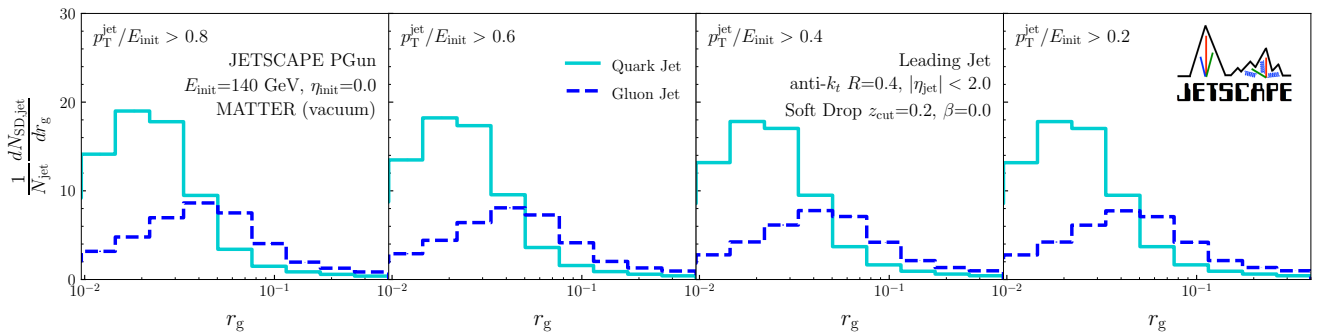


FIG. 7. Distributions of jet splitting momentum radius r_g normalized by the number of all triggered jets for the leading jets in events generated with PGUN. The jet shower evolution is performed by vacuum MATTER for the parent parton having a $E_{\text{init}} = 140$ GeV. Jets are reconstructed with $R = 0.4$ at midrapidity $|\eta_{\text{jet}}| < 2.0$. The results are shown for quark jets (solid) and gluon jets (dashed) with different p_T^{jet} triggers, 112, 84, 56, and 28 GeV. The Soft Drop parameters are $z_{\text{cut}} = 0.2$ and $\beta = 0$.

quark jets. For the jet cone size $R = 0.4$, almost no p_T^{jet} cut dependence can be observed in the vacuum case with fixed $E_{\text{init}} = 140$ GeV.

Figure 8 shows the modification of the r_g distribution

for the PGUN jets by the medium created in central Pb-Pb collisions at $\sqrt{s_{NN}} = 5.02$ TeV. For gluon jets, a monotonically decreasing trend with increasing r_g is observed in cases with a larger p_T^{jet} cut. Then, as the p_T^{jet} cut value

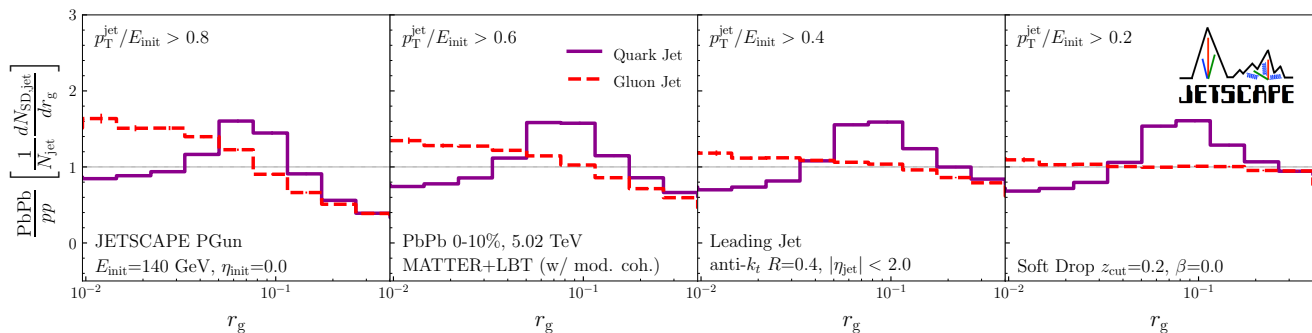


FIG. 8. Ratios of r_g distributions for the leading jets in events with the parent parton having a fixed initial energy $E_{\text{init}} = 140$ GeV generated by PGUN. The jet shower evolution in the QGP medium produced in 0%–10% Pb-Pb collisions at $\sqrt{s_{NN}} = 5.02$ TeV is performed by MATTER+LBT. All the setups are the same as in Fig. 2.

is reduced, the decrease rate becomes more gentle, and almost no modification can be seen for $p_T^{\text{jet}}/E_{\text{init}} > 0.2$. Thus, for gluon jets, the modification pattern is entirely brought by the effect from jet selection with p_T^{jet} cut than the actual structure modification of the hard splitting: Jets with an originally large splitting radius tend to have their constituents reach the edge of the jet cone more easily, making them lose more energy and thus less likely to be triggered.

The selection bias effect with p_T^{jet} cut can be observed also for quark jets as large- r_g suppression, with the same trend disappearing as the p_T^{jet} cut value is reduced. Additionally, in the case of quark jets, a prominent bump structure accompanied by slight suppression at small r_g is observed in the mid- r_g region. This feature is significantly different from that of gluon jets, providing evidence of direct modifications to the hard-splitting structure within quark jets.

To investigate the hard splitting modification in more detail, we show the MATTER-only results, in which the medium effect is turned off for $Q < 2$ GeV, in Fig. 9. For both quark jets and gluon jets, r_g distribution modification for any p_T^{jet} cut is nearly imperceptible. This indicates that the modifications observed in the full MATTER+LBT results are completely governed by the medium effect in the low-virtuality LBT phase.

In the case of quark jets, it is conceivable that hard splittings induced by the medium at low virtuality can have larger angles than those driven by virtuality. This might be attributed to the relatively lower initial virtuality in quark jets, where the virtuality-driven splittings are less likely to have very large angles. Such large-angle medium-induced splittings can be identified as hard branches by the SoftDrop grooming, subsequently manifesting in the r_g distribution as a shift from smaller r_g to moderate r_g (≈ 0.1), appearing as a bump structure in the full MATTER+LBT results. Conversely, for gluon jets, despite the presence of medium effects at low virtuality, splittings driven mainly by initial virtuality are still identified as hard branches by the Soft Drop grooming. The medium effects at low virtuality, which can involve large-

angle but soft radiation, do not alter the intrinsic hard structure of gluon jets while still resulting in significant jet energy loss.

In Fig. 10, r_g distributions for γ -tagged jets and inclusive jets in p - p collisions at $\sqrt{s} = 5.02$ TeV are compared. Unlike the case with z_g , both γ -tagged jets and inclusive jets exhibit a distinct p_T^{jet} dependency: narrowing as p_T^{jet} increases. This can lead to an additional contribution to the selection bias with p_T^{jet} cut in the presence of jet energy loss. Even without any modification on the splitting angle, the energy loss causes jets from parent partons with higher initial p_T , which typically exhibit narrower splittings, to be triggered more likely. As a result, narrowing of the r_g distribution is expected in the presence of the medium.

Furthermore, clear differences between γ -tagged jets and inclusive jets are also observed. Inclusive jets show a broader distribution since they have a larger fraction of gluon jets. As p_T^{jet} increases, this difference diminishes, owing to the decrease in the gluon jet fraction of inclusive jets.

The r_g distribution modifications for γ -tagged jets and inclusive jets in Pb-Pb collisions at $\sqrt{s_{NN}} = 5.02$ TeV are compared in Fig. 11. Here, it should be noted that two factors contribute to the energy loss selection bias effect of p_T^{jet} cut, causing the r_g narrowing irrelevant to the actual structural modification of hard splittings. Firstly, as confirmed by the results with a fixed E_{init} , jets with originally wider splittings tend to lose more energy, resulting in less triggered jets as r_g increases. In addition, as mentioned above for the p - p case, jets with parent partons with larger initial p_T , which possess the narrower r_g distribution, are triggered more likely in the presence of energy loss.

In the case of γ -tagged jets, at large r_g , the suppression due to the selection bias is evident for all the presented p_T^{jet} ranges. On the other hand, from small to mid r_g ($\lesssim 0.1$), the modification pattern is significantly flattened. This flat structure can predominantly be attributed to the large fraction of quark jets in γ -tagged jets: balance between the r_g broadening observed in

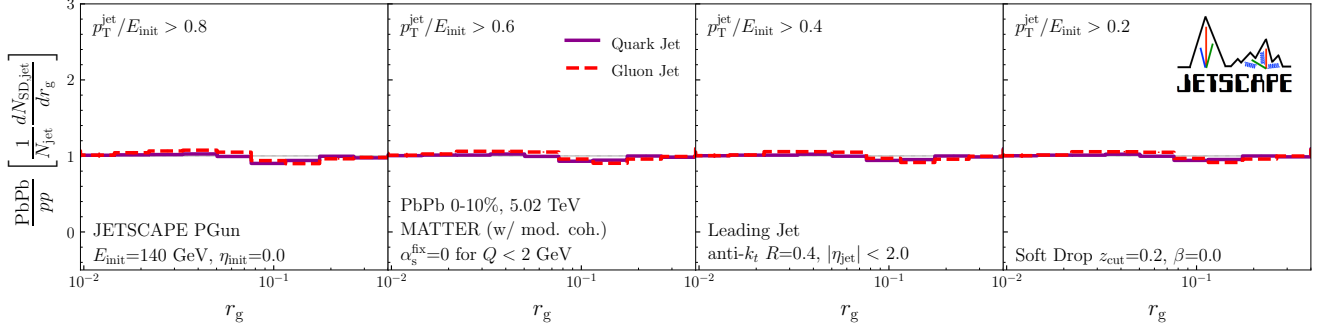


FIG. 9. Same as Fig. 8 for MATTER alone simulations, where the medium effect is turned off for jet partons with virtuality $Q < 2$ GeV.

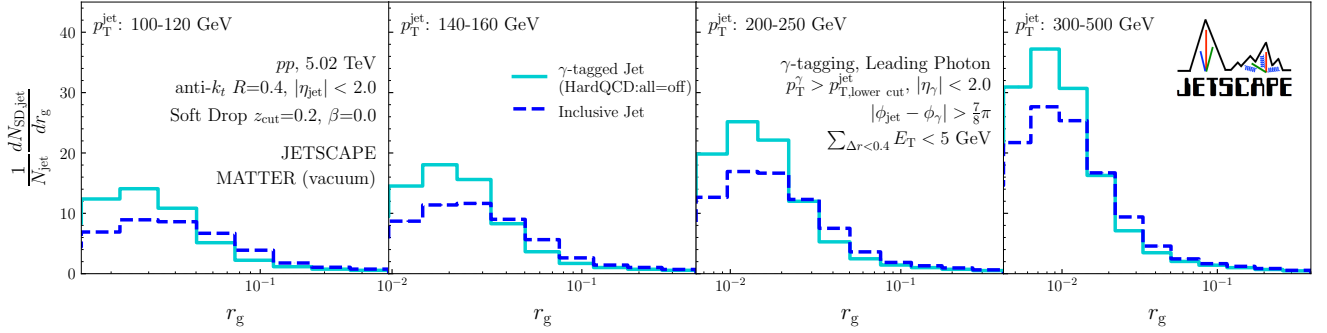


FIG. 10. Same as Fig. 7 for jets from hard scatterings in p - p collisions at $\sqrt{s} = 5.02$ TeV, generated by PYTHIAGUN with ISR and MPI. The results are shown for γ -tagged jets (solid) from prompt photon-generating hard processes (`HardQCD:all=off+PromptPhoton:all=on`) and inclusive jets (dashed) from inclusive hard processes (`HardQCD:all=on+PromptPhoton:all=on`) generated at leading order by PYTHIA 8 with different p_T^{jet} triggers. For γ -tagged jets, isolation requirement, relative azimuth angle cut, and the additional cut of $p_T^{jet} < p_T^\gamma$ are imposed.

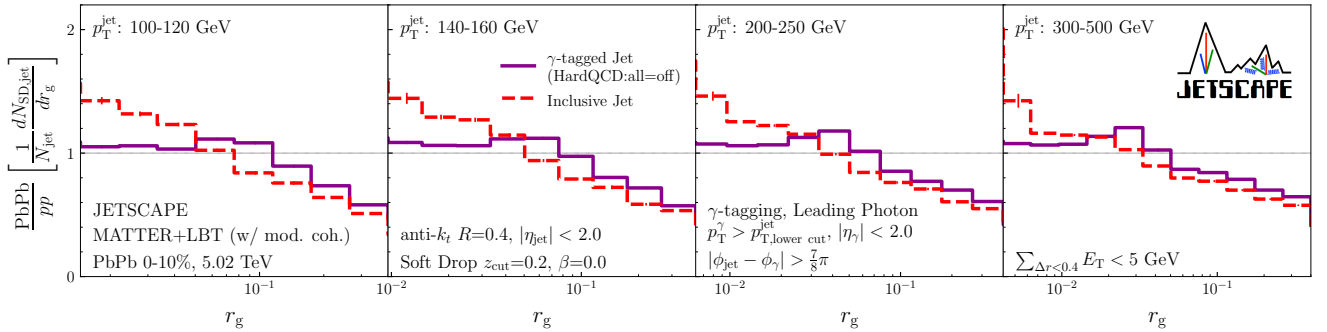


FIG. 11. Same as Fig. 8 for jets from hard scatterings at $\sqrt{s_{NN}} = 5.02$ TeV, generated by PYTHIAGUN with ISR and MPI. The results are shown for γ -tagged jets (solid) from prompt photon-generating hard processes (`HardQCD:all=off+PromptPhoton:all=on`) and inclusive jets (dashed) from inclusive hard processes (`HardQCD:all=on+PromptPhoton:all=on`) generated at leading order by PYTHIA 8 with different p_T^{jet} triggers. For γ -tagged jets, isolation requirement, relative azimuth angle cut, and the additional cut of $p_T^{jet} < p_T^\gamma$ are imposed.

quark jets and the selection bias effect. As p_T^{jet} increases, the broadening effect starts to slightly dominate, leading to subtle indications of a bump structure.

In the case of inclusive jets, across all presented p_T^{jet} ranges, the modification patterns are dominated by the

selection bias effect, exhibiting a monotonically decreasing trend with increasing r_g . This monotonic modification pattern in inclusive jets is consistent with those presented in our previous study [74], where our results show good agreement with experimental data from AL-

ICE [139] and ATLAS [140] simultaneously. Although the overall monotonic decreasing behavior remains, increasing the jet p_T^{jet} leads to a less steep slope at small r_g . This is attributed to the increase in the quark jet fraction, as seen in the narrowing of the r_g distribution in p - p collisions in Fig. 10

Figure 12 shows our prediction for the medium modification of the r_g distribution for γ -tagged jets in central Pb-Pb collisions at $\sqrt{s_{NN}} = 5.02$ TeV for different $x_{J\gamma}$ cuts. Unlike the z_g distribution, the r_g distribution exhibits a strong $x_{J\gamma}$ dependence. For the case with large $x_{J\gamma}$ cuts, the selection bias effect due to the r_g -dependence of energy loss appears prominently, resulting in a strong suppression at large r_g values. Here, it should be noted that the effect of the strong p_T^{jet} dependence on the r_g distribution of jets in vacuum is diminished, since, by setting an uppercut on p_T^{jet} , the feeddown from jets originating from parent partons with larger initial p_T is suppressed.

The selection bias effect is counterbalanced by the strong broadening effects on hard splittings, attributable to the large fraction of quark jets, in the small-to-mid r_g range. When the value of the lower $x_{J\gamma}$ cut is reduced to weaken the selection bias effect, the large r_g suppression diminishes, and concurrently, even a bump structure due to broadening emerges at mid r_g ($\lesssim 0.1$). This manifestation of the broadening effect in the r_g distribution represents a distinct characteristic of γ -tagged jets, contracting with the behavior of inclusive jets, where only a monotonous pattern entirely dominated by selection bias can be seen. Particularly, by varying the $x_{J\gamma}$ cut, one can control the selection bias effect and study the broadening effect more quantitatively. Therefore, γ -tagged jets provide a modification pattern in the r_g distribution that is more suitable for investigating structural modifications on the hard partonic splittings.

C. Relative transverse momentum of jet splittings

The relative transverse momentum of jet splittings,

$$k_{T,g} = p_{T,2} \sin r_g, \quad (10)$$

has recently been measured in experiments to investigate the transverse structure of hard splittings in jets [141]. We present the results of the $k_{T,g}$ distributions,

$$\frac{1}{N_{\text{jet}}} \frac{dN_{\text{SD,jet}}}{dk_{T,g}}, \quad (11)$$

for the vacuum PGUN jets in Fig. 13. Gluons are produced with greater virtuality than quarks, and thus, gluon jets exhibit a broader distribution with slightly larger values of $k_{T,g}$ than quark jets. Furthermore, no significant p_T^{jet} cut dependence can be seen in the vacuum case with fixed $E_{\text{init}} = 140$ GeV for the jet cone size $R = 0.4$.

The medium modifications in the $k_{T,g}$ distribution for the PGUN jets are shown in Fig. 14. In the results for

both quark and gluon jets, suppression at large $k_{T,g}$ values is seen. As seen in Eq. (10), $k_{T,g}$ increases with increasing r_g . Thus, one might naively think that this suppression is attributed to the same selection bias effect as in the r_g distribution: larger energy loss in jets with larger $k_{T,g}$. However, this is not only the cause, as evidenced by the persistence of the suppression at large- $k_{T,g}$ even when the p_T^{jet} cut is lowered to reduce the effect of hard splitting angle (r_g) dependence on energy loss. This suppression at large $k_{T,g}$ is actually brought also by the loss of $p_{T,2}$: large-angle soft radiations in the later stage can be trimmed by either the jet cone or the Soft Drop grooming.

The $p_{T,2}$ loss effect becomes apparent when focusing on the gluon jet with the smallest presented p_T^{jet} cut ($p_T^{\text{jet}}/E_{\text{init}} > 0.2$), taking into account the results of the r_g modification shown in Fig. 8. In this instance, whether due to energy loss effects or broadening, there is almost no modification observed in the r_g distribution of gluon jets. Thus, from Eq. (10), the modification in the $k_{T,g}$ must be attributed to the change in $p_{T,2}$, in particular, for the case with the small p_T^{jet} cut.

In the small to mid $k_{T,g}$ ($\lesssim 2$ GeV) region, similar to what was observed in the modification of the r_g distribution, a bump structure due to broadening is observed for quark jets. For the gluon jet case, the modification pattern is dominated by the effect of $p_{T,2}$ loss, with the r_g -dependence of jet energy loss also exerting a slight influence in cases of large p_T^{jet} cuts.

The modification on the $k_{T,g}$ from the MATTER alone simulations is shown in Fig. 15. By turning off the medium effect in the LBT phase, the loss of energy for the jet itself, as well as the $p_{T,2}$ loss, is significantly diminished, resulting in the disappearance of suppression at large $k_{T,g}$. Similar to what was observed in z_g and r_g distributions, the modification in the $k_{T,g}$ distribution is entirely governed by the medium effect in the low-virtuality LBT phase.

In Fig. 16, the comparison between the $k_{T,g}$ distributions for γ -tagged jets and inclusive jets in p - p collisions at $\sqrt{s} = 5.02$ TeV is shown for the same p_T^{jet} cuts. Inclusive jets exhibit a broader transverse momentum in hard splittings compared to γ -tagged jets, attributed to a larger gluon jet fraction, but this difference diminishes as p_T^{jet} increases.

Figure 17 presents the medium modification of the $k_{T,g}$ distribution for γ -tagged jets and inclusive jets. For both γ -tagged jets and inclusive jets, the overall modification exhibits a narrowing pattern mostly dominated by the $p_{T,2}$ loss of the prongs. Although no significant bump structure is observed, in the case of γ -tagged jets, a subtle indication of momentum-broadening effects on quark jets in the LBT phase can be discerned as a flattening on the small $k_{T,g}$ side.

Finally, the prediction for the $x_{J\gamma}$ -dependent medium modification of the $k_{T,g}$ distribution for γ -tagged jets in central Pb-Pb collisions at $\sqrt{s_{NN}} = 5.02$ TeV is shown in

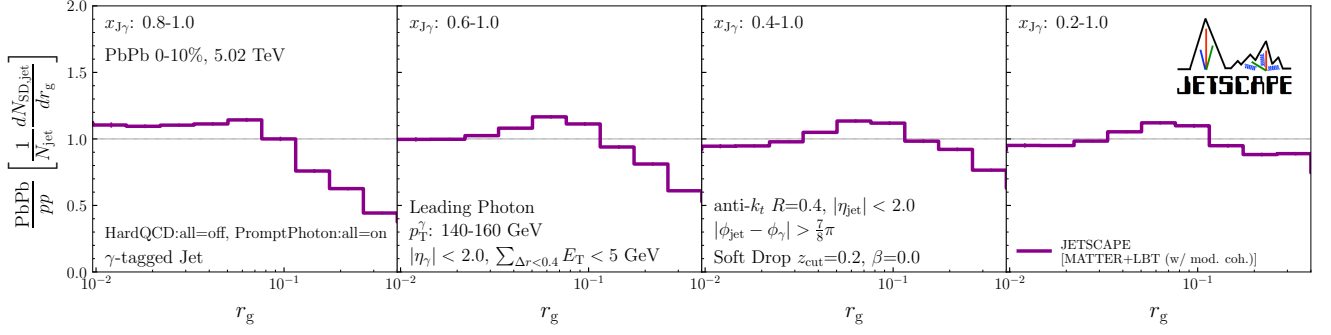


FIG. 12. Same as Fig. 8 for γ -tagged jets from prompt photon-generating hard processes (HardQCD:all=off+PromptPhoton:all=on) generated at leading order by PYTHIA 8 at $\sqrt{s_{NN}} = 5.02$ TeV for different $x_{J\gamma}$ ranges. The photon of $140 < p_T^\gamma < 160$ GeV is triggered with isolation requirement, relative azimuth angle cut.

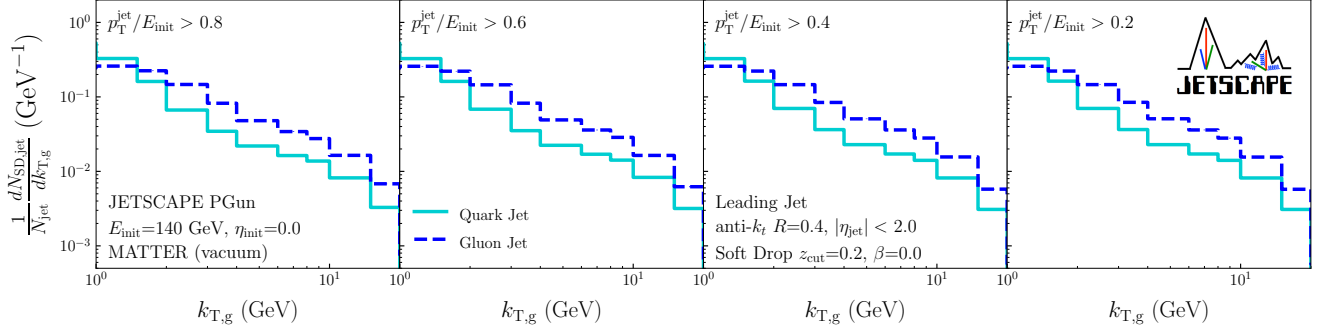


FIG. 13. Distributions of relative transverse momentum of jet splittings $k_{T,g}$ normalized by the number of all triggered jets for the leading jets in events generated with PGUN. The jet shower evolution is performed by vacuum MATTER for the parent parton having a $E_{init} = 140$ GeV. Jets are reconstructed with $R = 0.4$ at midrapidity $|\eta_{jet}| < 2.0$. The results are shown for quark jets (solid) and gluon jets (dashed) with different p_T^{jet} triggers, 112, 84, 56, and 28 GeV. The Soft Drop parameters are $z_{cut} = 0.2$ and $\beta = 0$.

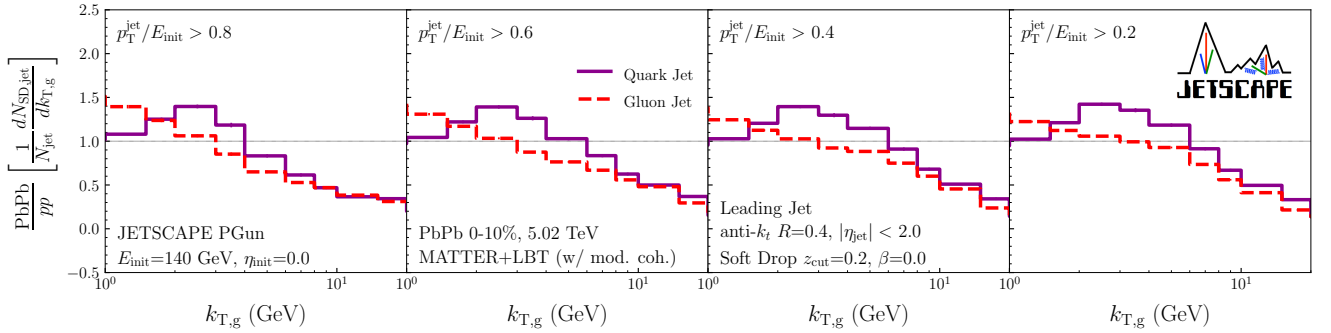


FIG. 14. Ratios of $k_{T,g}$ distributions for the leading jets in events with the parent parton having a fixed initial energy $E_{init} = 140$ GeV generated by PGUN. The jet shower evolution in the QGP medium produced in 0%–10% Pb-Pb collisions at $\sqrt{s_{NN}} = 5.02$ TeV is performed by MATTER+LBT. All the setups are the same as in Fig. 2.

Fig. 18. Given that the suppression at large $k_{T,g}$ persists even with a reduced $x_{J\gamma}$ cut ($x_{J\gamma} > 0.2$), it is evident that jets with large $k_{T,g}$ cannot recover, even when jets with significant energy loss are included, due to the presence of $p_{T,2}$ loss. On the small $k_{T,g}$ side, a very flat pattern is seen as a consequence of the competition be-

tween the transverse momentum broadening of quark jets in LBT and the other effects narrowing the distribution.

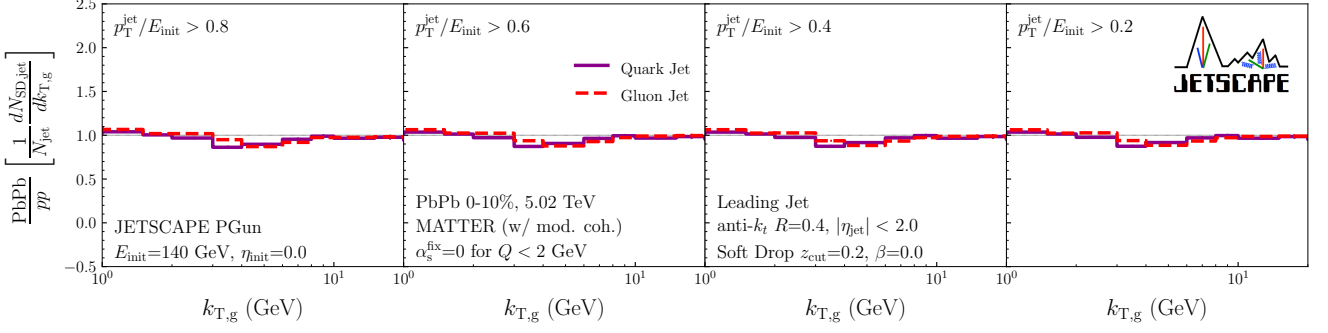


FIG. 15. Same as Fig. 14 for MATTER alone simulations, where the medium effect is turned off for jet partons with virtuality $Q < 2$ GeV.

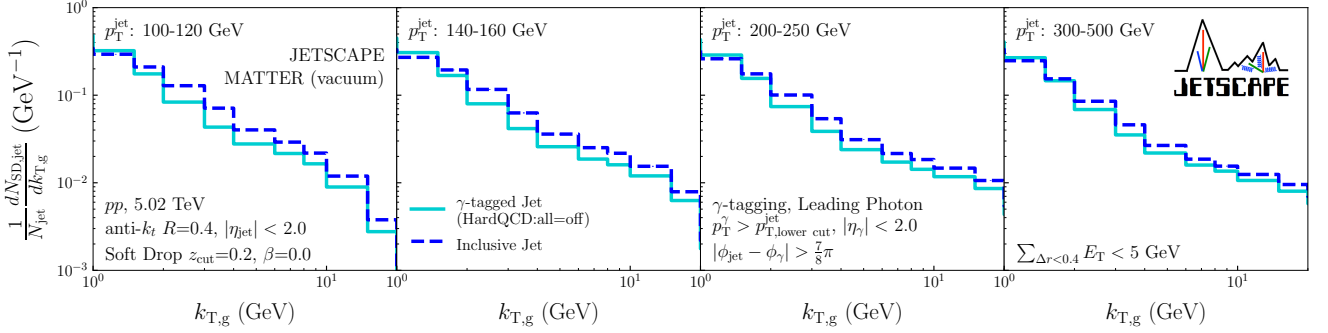


FIG. 16. Same as Fig. 13 for jets from hard scatterings in p - p collisions at $\sqrt{s} = 5.02$ TeV, generated by PYTHIAGUN with ISR and MPI. The results are shown for γ -tagged jets (solid) from prompt photon-generating hard processes (`HardQCD:all=off+PromptPhoton:all=on`) and inclusive jets (dashed) from inclusive hard processes (`HardQCD:all=on+PromptPhoton:all=on`) generated at leading order by PYTHIA 8 with different p_T^{jet} triggers. For γ -tagged jets, isolation requirement, relative azimuth angle cut, and the additional cut of $p_T^{\text{jet}} < p_T^{\gamma}$ are imposed.

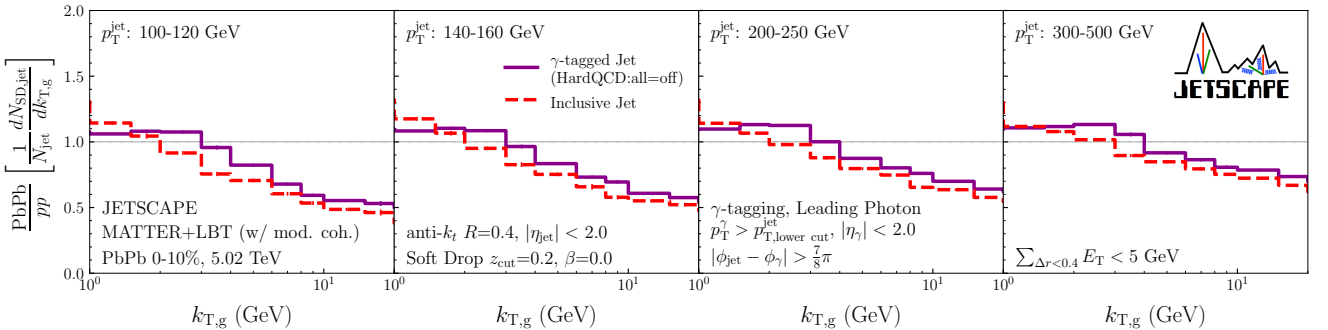


FIG. 17. Same as Fig. 14 for jets from hard scatterings at $\sqrt{s_{NN}} = 5.02$ TeV, generated by PYTHIAGUN with ISR and MPI. The results are shown for γ -tagged jets (solid) from prompt photon-generating hard processes (`HardQCD:all=off+PromptPhoton:all=on`) and inclusive jets (dashed) from inclusive hard processes (`HardQCD:all=on+PromptPhoton:all=on`) generated at leading order by PYTHIA 8 with different p_T^{jet} triggers. For γ -tagged jets, isolation requirement, relative azimuth angle cut, and the additional cut of $p_T^{\text{jet}} < p_T^{\gamma}$ are imposed.

D. Groomed jet mass

Finally, we investigate the medium modification of the groomed jet mass distribution,

$$\frac{1}{N_{\text{jet}}} \frac{dN_{\text{SD,jet}}}{dm_g}, \quad (12)$$

where the groomed jet mass is defined as

$$m_g = \sqrt{(p_1^0 + p_2^0)^2 - (\vec{p}_1 + \vec{p}_2)^2}. \quad (13)$$

In Fig. 19, the m_g distributions for the vacuum PGUN

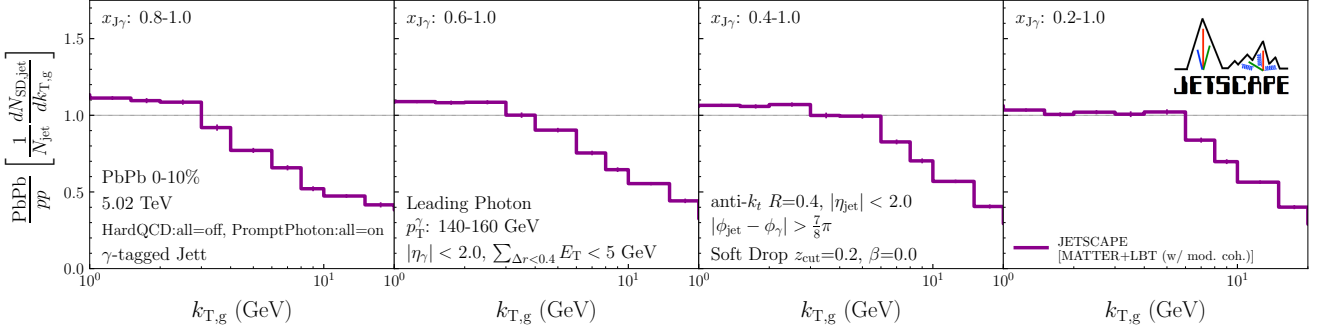


FIG. 18. Same as Fig. 14 for γ -tagged jets from prompt photon-generating hard processes (HardQCD:all=off+PromptPhoton:all=on) generated at leading order by PYTHIA 8 at $\sqrt{s_{NN}} = 5.02$ TeV for different $x_{J,\gamma}$ ranges. The photon of $140 < p_T^\gamma < 160$ GeV is triggered with isolation requirement, relative azimuth angle cut.

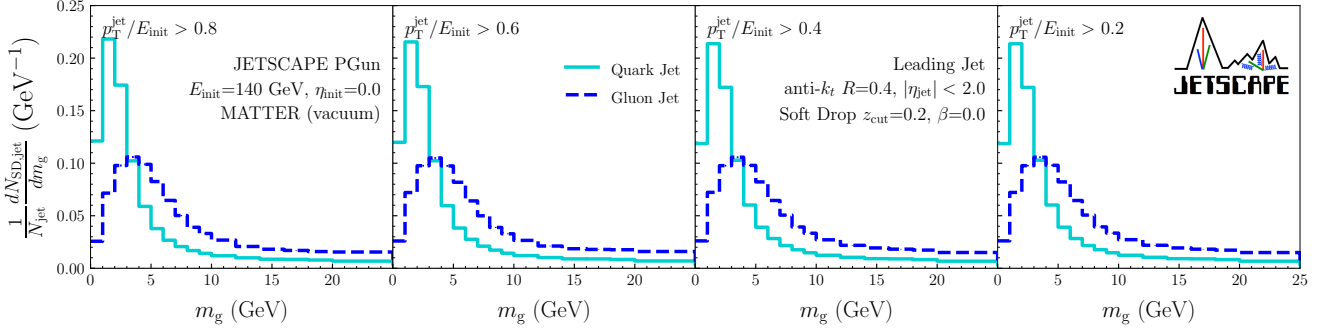


FIG. 19. Distributions of the relative transverse momentum of jet splittings m_g normalized by the number of all triggered jets for the leading jets in events generated with PGUN. The jet shower evolution is performed by vacuum MATTER for the parent parton having a $E_{\text{init}} = 140$ GeV. Jets are reconstructed with $R = 0.4$ at midrapidity $|\eta_{\text{jet}}| < 2.0$. The results are shown for quark jets (solid) and gluon jets (dashed) with different p_T^{jet} triggers, 112, 84, 56, and 28 GeV. The Soft Drop parameters are $z_{\text{cut}} = 0.2$ and $\beta = 0$.

jets are shown. Here, again, due to the larger virtuality at the initial hard scattering production, gluon jets have a broader distribution with larger m_g than quark jets. For the vacuum case with fixed $E_{\text{init}} = 140$ GeV, no significant p_T^{jet} cut dependence is seen for the jet cone size $R = 0.4$.

The medium modification of m_g distribution for jets from the PGUN simulations with fixed E_{init} is shown in Fig. 20. In the case of quark jets, a clear bump structure is observed due to the shift of small m_g to mid m_g caused by medium effects. On the other hand, such behavior is not observed for gluon jets, which exhibit a monotonic trend. Besides, for both quark and gluon jets with large p_T^{jet} cuts, suppression at large m_g is observed, attributed to the greater energy loss in jets with larger masses, which results in wider splittings. Then, with the small p_T^{jet} cuts, the suppression becomes slightly moderate at mid m_g (≈ 10 – 15 GeV), yet still dominates the modification. This is because, analogous to the case for $k_{T,g}$, the jet energy loss—primarily due to large-angle energy emission outside of the jet cone—results in the loss of m_g .

In Fig. 21, the modification by the MATTER alone simu-

lations is shown. Also, through m_g distribution, it can be confirmed that no significant modification in the structure of jet hard splittings at high virtuality occurs for both gluon jets and quark jets. Thus, the modification pattern is entirely brought about by the evolution at low virtuality.

The m_g distributions for γ -tagged jets and inclusive jets in p - p collisions at $\sqrt{s} = 5.02$ TeV are compared in Fig. 22. The inclusive jet results exhibit a broader distribution in the m_g due to the larger gluon jet fraction, but the difference diminishes as p_T^{jet} increases, similarly to the r_g and $k_{T,g}$ distributions. The medium modification is shown in Fig. 23. For inclusive jets, the modification pattern is dominated by the shift towards smaller m_g , attributed to larger energy loss with wider angle profiles, and does not show any clear manifestation of mass gain for the hard splittings. In the case of γ -tagged jets, a bump due to the mass gain for quark jets in the LBT phase appears on the small m_g side, while a similar suppression to that of inclusive jets is observed at large m_g .

We present our prediction for the $x_{J,\gamma}$ -dependent medium modification of the m_g distribution for γ -tagged

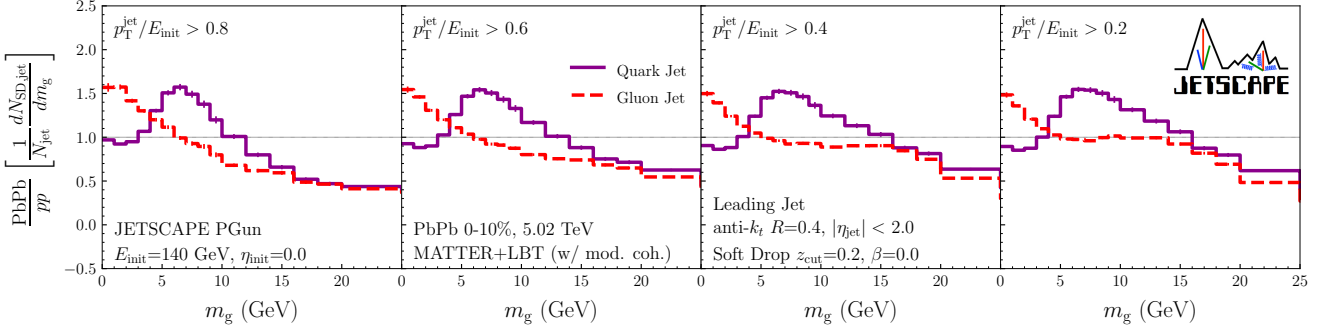


FIG. 20. Ratios of m_g distributions for the leading jets in events with the parent parton having a fixed initial energy $E_{\text{init}} = 140$ GeV generated by PGUN. The jet shower evolution in the QGP medium produced in 0%–10% Pb-Pb collisions at $\sqrt{s_{NN}} = 5.02$ TeV is performed by MATTER+LBT. All the setups are the same as in Fig. 2.

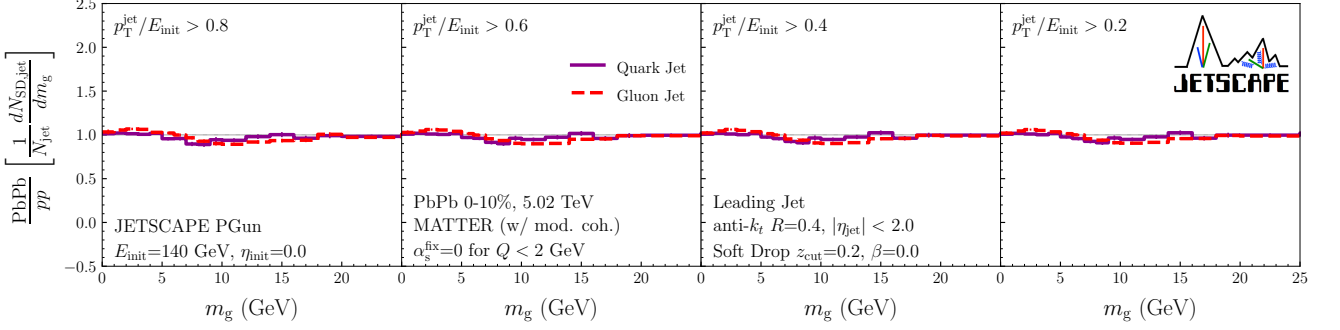


FIG. 21. Same as Fig. 20 for MATTER alone simulations, where the medium effect is turned off for jet partons with virtuality $Q < 2$ GeV.

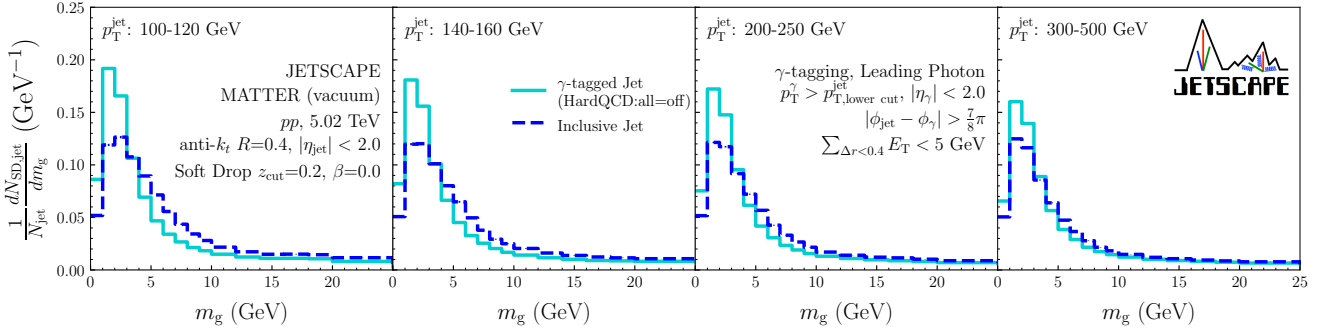


FIG. 22. Same as Fig. 19 for jets from hard scatterings in p - p collisions at $\sqrt{s} = 5.02$ TeV, generated by PYTHIAGUN with ISR and MPI. The results are shown for γ -tagged jets (solid) from prompt photon-generating hard processes (`HardQCD:all=off+PromptPhoton:all=on`) and inclusive jets (dashed) from inclusive hard processes (`HardQCD:all=on+PromptPhoton:all=on`) generated at leading order by PYTHIA 8 with different p_T^{jet} triggers. For γ -tagged jets, isolation requirement, relative azimuth angle cut, and the additional cut of $p_T^{\text{jet}} < p_T^{\gamma}$ are imposed.

jets in Fig. 24. A bump structure associated with mass gain from the medium is observed in hard splittings. At large m_g , jets with larger masses experience greater energy loss, leading to wider splittings and suppression at large $x_{J\gamma}$ cuts. Reducing the $x_{J\gamma}$ cut includes contributions from jets with significant energy loss, weakening the suppression, but it persists even at the smallest $x_{J\gamma}$

cut ($x_{J\gamma} > 0.2$). This is attributed to the loss of m_g caused by energy emitted at large angles outside the jet cone or soft components groomed away by the Soft Drop procedure.

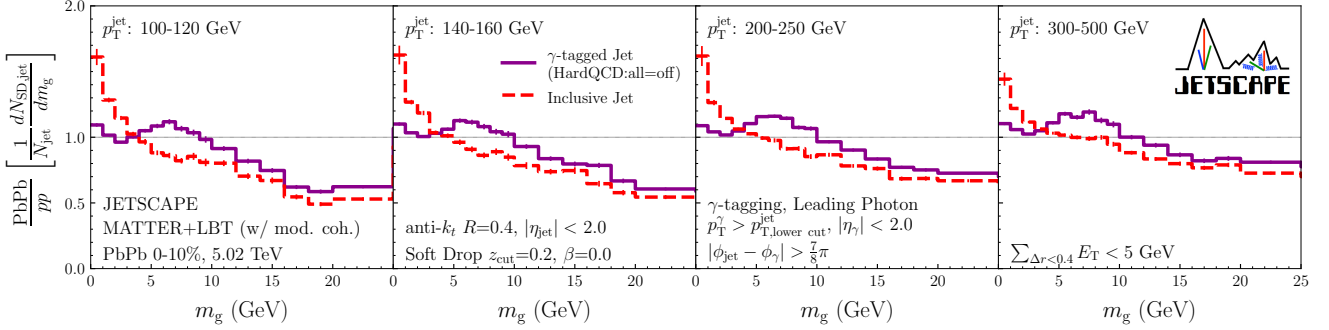


FIG. 23. Same as Fig. 20 for jets from hard scatterings at $\sqrt{s_{NN}} = 5.02$ TeV, generated by PYTHIAGUN with ISR and MPI. The results are shown for the inclusive jets (dashed) from inclusive hard processes (`HardQCD:all=on+PromptPhoton:all=on`) and γ -tagged jets (solid) from prompt photon-generating hard processes (`HardQCD:all=off+PromptPhoton:all=on`) generated at leading order by PYTHIA 8 with different p_T^{jet} triggers. For γ -tagged jets, isolation requirement, relative azimuth angle cut, and the additional cut of $p_T^{\text{jet}} < p_T^{\gamma}$ are imposed.

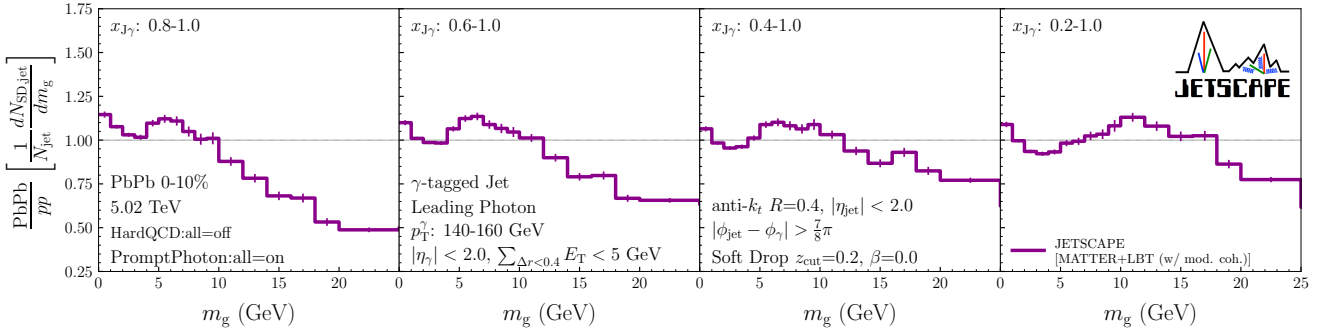


FIG. 24. Same as Fig. 20 for γ -tagged jets from prompt photon-generating hard processes (`HardQCD:all=off+PromptPhoton:all=on`) generated at leading order by PYTHIA 8 at $\sqrt{s_{NN}} = 5.02$ TeV for different $x_{J\gamma}$ ranges. The photon of $140 < p_T^{\gamma} < 160$ GeV is triggered with isolation requirement, relative azimuth angle cut.

V. COMPARISON WITH EXPERIMENTAL DATA

1. Relative transverse momentum of jet splittings

In this section, we compare our analysis results, using the same event set of JETSCAPE simulations as in the previous section, with existing experimental data from the LHC for benchmarking. Additionally, we note that similar comparisons with experimental results, using the same parameter settings and configurations, have also been detailed in our previous work [74].

A. Inclusive jet substructure

In this subsection, we present the results of groomed observables for inclusive jets. The initial hard processes for the simulations were generated using the PYTHIAGUN module with `HardQCD:all=on`.

The distributions of $k_{T,g}$ obtained from Soft Drop and dynamical grooming [64], in p - p collisions are shown in Fig. 25, and their modifications in Pb-Pb collisions at $\sqrt{s_{NN}} = 5.02$ TeV are presented in Fig. 26. The results from our JETSCAPE simulations are compared with the experimental results from ALICE [56].

The Soft Drop and dynamical grooming results from the JETSCAPE PP19 tune show consistency with experimental data for the $k_{T,g}$ distribution in p - p collisions, remaining within the uncertainty range. For Pb-Pb collisions, the modification in the distributions aligns with the inclusive full jet results presented in the main text, demonstrating a monotonically decreasing behavior as a function of $k_{T,g}$, which is primarily governed by selection bias by the p_T cut and the loss of $p_{T,2}$. They successfully capture the experimental trends, while dynamical grooming results exhibit slight over-suppression. Notably, the Soft Drop results are in excellent agreement with experimental data within the uncertainties.

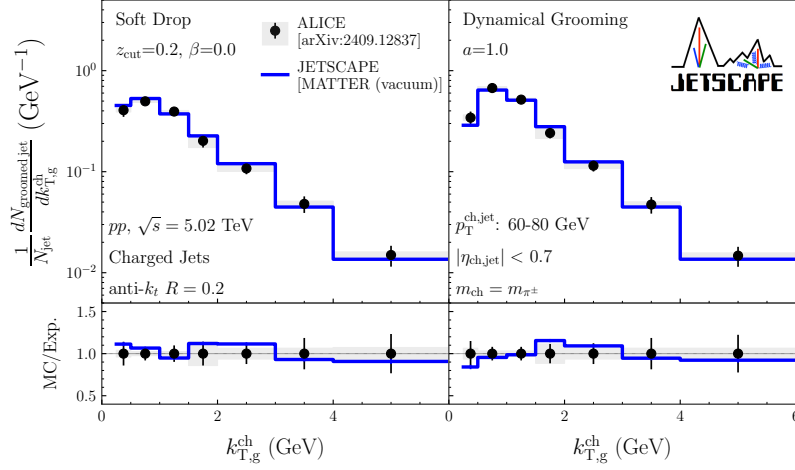


FIG. 25. Distributions of the relative transverse momentum of jet splittings, $k_{T,g}$ for charged jets with $60 < p_T^{\text{ch,jet}} < 80$ GeV and $|\eta_{\text{ch,jet}}| < 0.7$, using $R = 0.2$ in p - p collisions at $\sqrt{s} = 5.02$ TeV, and the ratios for different grooming algorithms: Soft Drop with $z_{\text{cut}} = 0.2$ and $\beta = 0$ (left), and dynamical grooming with $a = 1.0$ (right). The solid lines and circles with statistical error bars show the results from vacuum MATTER of JETSCAPE and the experimental data from the ALICE Collaboration [56], respectively. The bands indicate the systematic uncertainties of the experimental data.

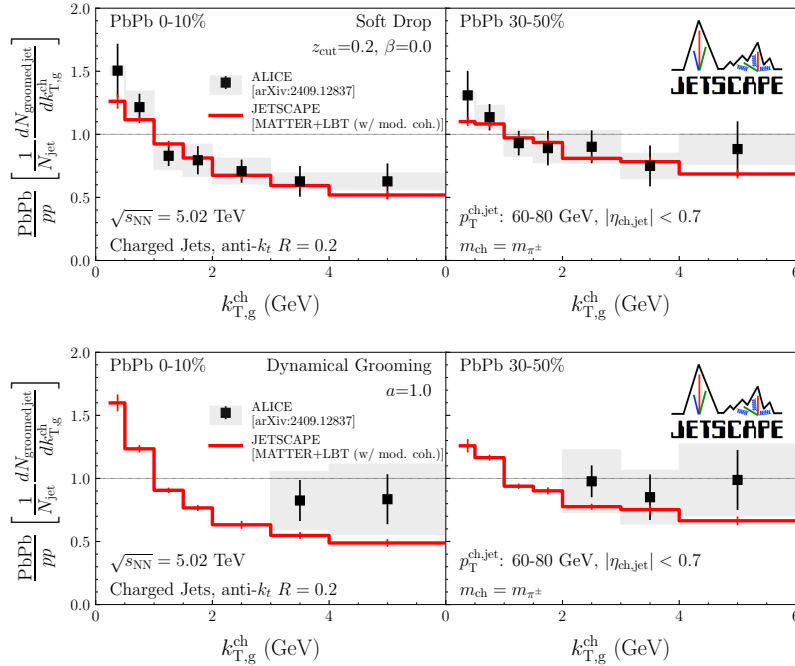


FIG. 26. Ratios of $k_{T,g}$ distributions between Pb-Pb and p - p collisions at $\sqrt{s_{NN}} = 5.02$ TeV for charged jets with $60 < p_T^{\text{ch,jet}} < 80$ GeV and $|\eta_{\text{ch,jet}}| < 0.7$, using $R = 0.2$ for different centralities, 0%–10% (left) and 30%–50% (right), and grooming algorithms, Soft Drop with $z_{\text{cut}} = 0.2$ and $\beta = 0$ (upper) and dynamical grooming with $a = 1.0$ (lower). The solid lines and squares with statistical error bars show the results from MATTER+LBT of JETSCAPE and the experimental data from the ALICE Collaboration [56], respectively. The bands indicate the systematic uncertainties of the experimental data.

2. Groomed Jet Mass

Here, we present a comparison of our results for Soft Drop groomed jet mass m_g with experimental results. The comparison of the unfolded m_g/p_T distribution for

full jets with $R = 0.4$ in p - p collisions from CMS [45] is shown in Fig. 27, while the comparison of the m_g distribution for charged jets with $R = 0.2$ in p - p collisions from ALICE [57] is shown in Fig. 28. The results for p - p collisions are in agreement with the experimen-

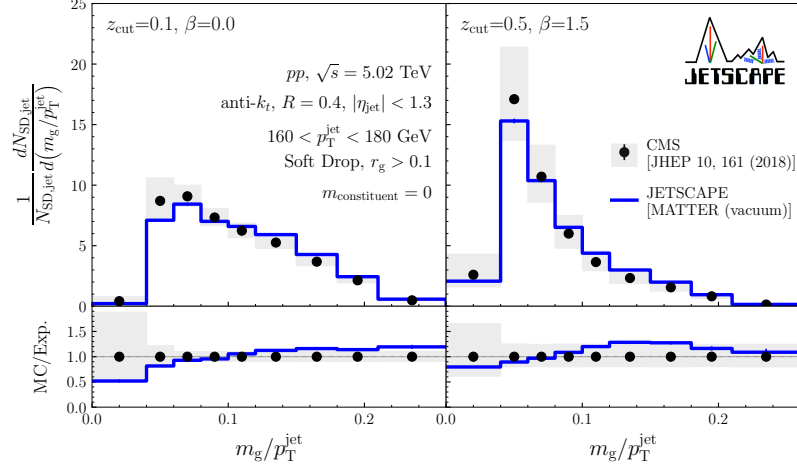


FIG. 27. Distributions of the ratio of the Soft Drop groomed jet mass to the jet transverse momentum, m_g/p_T^{jet} , for full jets with $160 < p_T^{\text{jet}} < 180$ GeV and $|\eta_{\text{jet}}| < 1.3$, using $R = 0.4$ in p - p collisions at $\sqrt{s} = 5.02$ TeV for different grooming parameters: $z_{\text{cut}} = 0.1$ and $\beta = 0$ (left), and $z_{\text{cut}} = 0.5$ and $\beta = 1.5$ (right). The solid lines and circles with statistical error bars show the results from vacuum MATTER of JETSCAPE and the unfolded experimental data from the CMS Collaboration [45], respectively. The bands indicate the systematic uncertainties of the experimental data.

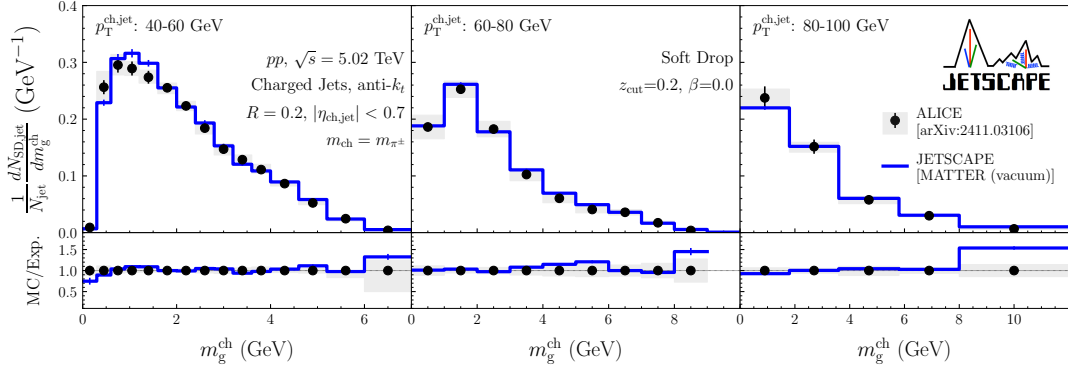


FIG. 28. Distributions of the Soft Drop groomed mass, m_g for charged jets with $R = 0.2$ and $|\eta_{\text{ch,jet}}| < 0.7$ in p - p collisions at $\sqrt{s} = 5.02$ TeV, and the ratios for different $p_T^{\text{ch,jet}}$ range. The Soft Drop parameters are $z_{\text{cut}} = 0.2$ and $\beta = 0$. The solid lines and circles with statistical error bars show the results from vacuum MATTER of JETSCAPE and the experimental data from the ALICE Collaboration [57], respectively. The bands indicate the systematic uncertainties of the experimental data.

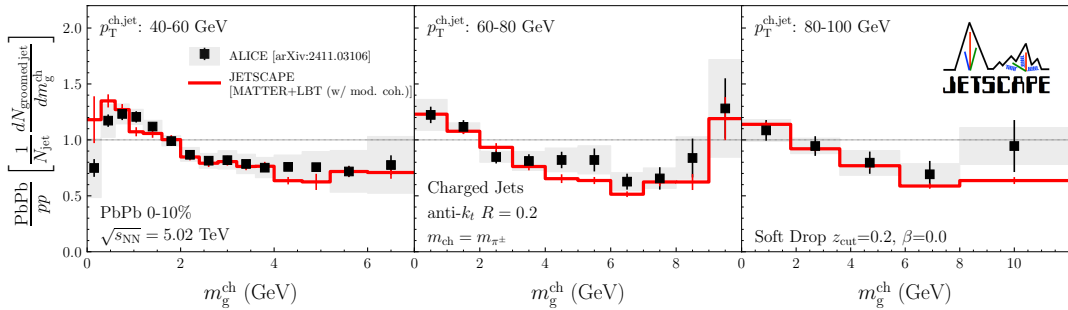


FIG. 29. Ratios of Soft Drop m_g distributions between 0%–10% Pb-Pb and p - p collisions at $\sqrt{s_{\text{NN}}} = 5.02$ TeV for charged jets with $R = 0.2$ and $|\eta_{\text{ch,jet}}| < 0.7$ for different $p_T^{\text{ch,jet}}$ range. The Soft Drop parameters are $z_{\text{cut}} = 0.2$ and $\beta = 0$. The solid lines and squares with statistical error bars show the results from MATTER+LBT of JETSCAPE and the experimental data from the ALICE Collaboration [57], respectively. The bands indicate the systematic uncertainties of the experimental data.

tal data within the uncertainty range, except for regions with significantly low jet counts, such as the tails of the

distributions. It should be noted that, while our calculations are based on Monte Carlo simulations, the masses of jet constituents were adjusted to align with experimental methodologies: massless for comparison with CMS data and the charged pion mass for comparison with ALICE data. This adjustment, while necessary to match experimental analysis techniques, has a non-negligible impact on the results, leading to noticeable changes in the distributions.

Figure 29 shows the modifications of the Soft Drop groomed jet mass distributions in 0%–10% Pb-Pb collisions, compared with the ALICE data [57]. As with the inclusive full jet results presented in the main text, the behavior is dominated by the p_T^{jet} cut-induced selection bias and the loss of prong mass, leading to suppression at large m_g . The results capture the experimental trends and agree with the data within the uncertainty range across most m_g regions. A slight enhancement observed in some p_T^{jet} ranges for the largest m_g bin is primarily attributed to the very low jet counts in the tail of the distribution, particularly in p - p collisions.

B. Jet splitting radius of γ -tagged jet

Here, we present the results for the jet splitting radius r_g of γ -tagged jets from simulations conducted using the PYTHIAGUN module with `HardQCD:all=off` and `PromptPhoton:all=on`. Figures 30 and 31 present comparisons with CMS data [55] for r_g distributions in p - p collisions and their modifications in 0%–30% Pb-Pb collisions, respectively. Results are shown for two lower cuts on $x_{J\gamma}$: 0.8 and 0.4. For p - p collisions, the distributions obtained from the vacuum MATTER calculations are narrower than the experimental data for both $x_{J\gamma}$ cut values. This behavior is consistent with the trends observed in other Monte Carlo model calculations compared in Ref. [55].

For the Pb-Pb results, at $x_{J\gamma} > 0.8$, suppression at large r_g region, attributed to selection bias, is observed, similar to the inclusive jet results presented in the main text and in our previous study [74], as well as the γ -tagged jet results with large $x_{J\gamma}$ cuts in the main text. While there is a sizable quantitative difference compared to the experimental data, the results qualitatively reproduce the observed trends.

On the other hand, for $x_{J\gamma} > 0.4$, as investigated in the $x_{J\gamma}$ dependence presented in the main text, the effect of selection bias is mitigated, leading to the disappearance of the suppression in the large r_g region. This behavior closely matches the experimental observations. Furthermore, as discussed in the main text, the strong modification in splitting structures, such as the pronounced bump associated with the dominance of quark jets, are not clearly visible with the current binning resolution. Future measurements with higher precision are anticipated to reveal this feature more distinctly.

VI. SUMMARY

In this work, we investigated medium modifications in jet substructure observables from Soft Drop grooming, including the jet splitting momentum fraction (z_g), splitting radius (r_g), relative transverse momentum of splittings ($k_{T,g}$), and groomed jet mass (m_g), in 0%–10% Pb-Pb collisions at $\sqrt{s_{NN}} = 5.02$ TeV. These analyses utilized the MATTER+LBT multistage jet evolution model within the JETSCAPE framework, using the JETSCAPEv3.5 AA22 tune [89], as employed in previous studies [74, 90]. In particular, this effort should be compared to the closely related earlier companion paper Ref. [93], which studied medium effects on γ -triggered jets. For the initial hard processes, events were generated with different configurations to isolate specific effects, primarily from the flavor of the parent partons, energy loss, and the selection bias introduced by the p_T trigger.

The PGUN simulations, in which a single hard parton with specified initial energy and flavor (light quark or gluon) evolves through shower development, revealed a clear flavor dependence in medium modifications to r_g , $k_{T,g}$, and m_g , with quark jets exhibiting distinct bump structures that are absent in gluon jets. This contrast arises from the narrow initial structure of quark jets, which allows medium effects to induce larger splittings, whereas the hard, vacuum-like branching of gluon jets remains largely unaffected. The PGUN results also highlight the selection bias, which dominates inclusive jet measurements and suppresses jets with broader structures. Lowering the p_T^{jet} cut mitigates this effect, fully eliminating the suppression in r_g distributions and partially reducing it in $k_{T,g}$ and m_g distributions. These medium modifications were found to originate predominantly at low virtuality ($Q < 2$ GeV).

We also presented predictions for γ -tagged jets by performing simulations with the MATTER+LBT setup within the JETSCAPE framework, incorporating a realistic initial hard process generated by PYTHIA 8. These simulations revealed clear medium-induced broadening in r_g , $k_{T,g}$, and m_g . Unlike inclusive jets, which exhibited smooth, monotonic suppression dominated by selection bias, γ -tagged jets displayed a flat structure at small r_g and $k_{T,g}$ and a distinct bump in m_g , amplified by their quark-jet-dominated nature. Further analysis demonstrated that lowering the $x_{J\gamma}$ cut for γ -tagged jets effectively reduced selection bias, making the intrinsic modifications more apparent. This study underscores the utility of γ -tagged jets, and similarly Z -tagged jets, as powerful probes for disentangling medium effects on the jet substructure and advancing our understanding of jet-QGP medium interactions in high-energy heavy-ion collisions. When these observables are eventually measured in experiments at high precision, incorporating them into Bayesian analyses with theoretical models could significantly constrain parameters associated with the fundamental mechanisms of jet-QGP medium interactions.

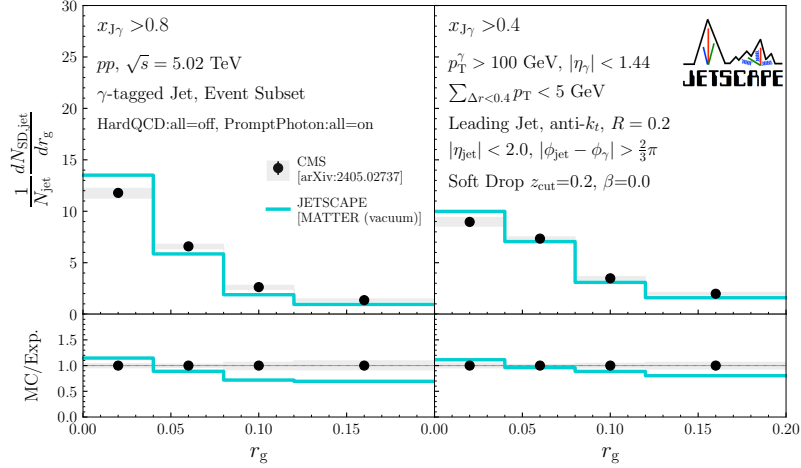


FIG. 30. Distributions of the Soft Drop groomed mass, r_g for γ -tagged jets with $R = 0.2$ in p - p collisions at $\sqrt{s} = 5.02$ TeV, and the ratios for $x_{J\gamma} > 0.8$ (left) and $x_{J\gamma} > 0.4$ (right). Leading full jets within $|\eta_{\text{jet}}| < 2$ and $|\phi_{\text{jet}} - \phi_\gamma| > 2\pi/3$ are paired with isolated photons satisfying $p_T^\gamma > 100$ GeV and $|\eta_\gamma| < 1.44$ as the trigger condition. The Soft Drop parameters are $z_{\text{cut}} = 0.2$ and $\beta = 0$. The solid lines and circles with statistical error bars show the results from vacuum MATTER of JETSCAPE and the experimental data from the CMS Collaboration [55], respectively. The bands indicate the systematic uncertainties of the experimental data.

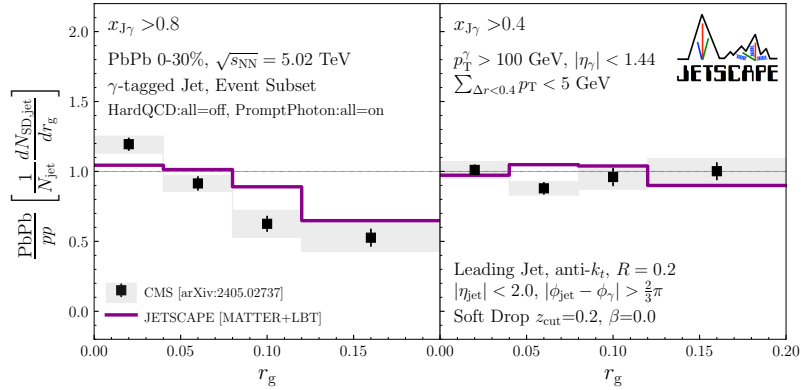


FIG. 31. Ratios of Soft Drop r_g distributions between 0%–30% Pb-Pb and p - p collisions at $\sqrt{s_{NN}} = 5.02$ TeV. Full jets of highest p_T^{jet} within $|\eta_{\text{jet}}| < 2$ and $|\phi_{\text{jet}} - \phi_\gamma| > 2\pi/3$ are paired with isolated photons satisfying $p_T^\gamma > 100$ GeV and $|\eta_\gamma| < 1.44$ as the trigger condition. The Soft Drop parameters are $z_{\text{cut}} = 0.2$ and $\beta = 0$. The solid lines and squares with statistical error bars show the results from MATTER+LBT of JETSCAPE and the experimental data from the CMS Collaboration [55], respectively. The bands indicate the systematic uncertainties of the experimental data.

ACKNOWLEDGMENTS

This work was supported in part by the National Science Foundation (NSF) within the framework of the JETSCAPE collaboration, under grant number OAC-2004571 (CSSI:X-SCAPE). It was also supported under PHY-1516590 and PHY-1812431 (R.J.F., M.Ko., C.P. and A.S.); it was supported in part by the US Department of Energy, Office of Science, Office of Nuclear Physics under grant numbers DE-AC02-05CH11231 (X.-N.W. and W.Z.), DE-AC52-07NA27344 (A.A., R.A.S.), DE-SC0013460 (A.K., A.M., C.Sh., I.S., C.Si and R.D.), DE-SC0021969 (C.Sh. and W.Z.), DE-SC0024232 (C.Sh.

and H.R.), DE-SC0012704 (B.S.), DE-FG02-92ER40713 (J.H.P. and M.Ke.), DE-FG02-05ER41367 (C.Si, D.S. and S.A.B.), DE-SC0024660 (R.K.E), DE-SC0024347 (J.-F.P. and M.S.). The work was also supported in part by the National Science Foundation of China (NSFC) under grant numbers 11935007, 11861131009 and 11890714 (Y.H. and X.-N.W.), by the Natural Sciences and Engineering Research Council of Canada (C.G., S.J., and G.V.), by the University of Regina President's Tri-Agency Grant Support Program (G.V.), by the Canada Research Chair program (G.V. and A.K.) reference number CRC-2022-00146, by the Office of the Vice President for Research (OVPR) at Wayne State University (Y.T.),

by JSPS KAKENHI Grant No. 22K14041 (Y.T.), and by the São Paulo Research Foundation (FAPESP) under projects 2016/24029-6, 2017/05685-2 and 2018/24720-6 (M.L.). C.Sh., J.-F.P., and R.K.E. acknowledge a DOE Office of Science Early Career Award. I. S. was funded as part of the European Research Council project ERC-2018-ADG-835105 YoctoLHC, and as a part of the Center of Excellence in Quark Matter of the Academy of Finland (project 346325).

Calculations for this work used the Wayne State Grid, generously supported by the Office of the Vice President of Research (OVPR) at Wayne State University. The bulk medium simulations were performed using resources provided by the Open Science Grid (OSG) [142, 143], which is supported by the National Science Foundation award #2030508. Data storage was provided in part by the OSIRIS project supported by the National Science Foundation under grant number OAC-1541335.

-
- [1] J. D. Bjorken, Energy loss of energetic partons in quark-gluon plasma: Possible extinction of high $p(t)$ jets in hadron-hadron collisions, Fermilab, Report No. FERMILAB-PUB-82-059-THY (unpublished).
- [2] D. A. Appel, Jets as a Probe of Quark - Gluon Plasmas, *Phys. Rev. D* **33**, 717 (1986).
- [3] R. Baier, Y. L. Dokshitzer, A. H. Mueller, S. Peigne, and D. Schiff, Radiative energy loss of high-energy quarks and gluons in a finite volume quark - gluon plasma, *Nucl. Phys. B* **483**, 291 (1997), [arXiv:hep-ph/9607355](#).
- [4] R. Baier, Y. L. Dokshitzer, A. H. Mueller, S. Peigne, and D. Schiff, Radiative energy loss and $p(T)$ broadening of high-energy partons in nuclei, *Nucl. Phys. B* **484**, 265 (1997), [arXiv:hep-ph/9608322](#).
- [5] B. G. Zakharov, Fully quantum treatment of the Landau-Pomeranchuk-Migdal effect in QED and QCD, *JETP Lett.* **63**, 952 (1996), [arXiv:hep-ph/9607440](#).
- [6] M. Gyulassy, P. Levai, and I. Vitev, Jet quenching in thin quark gluon plasmas. 1. Formalism, *Nucl. Phys. B* **571**, 197 (2000), [arXiv:hep-ph/9907461](#).
- [7] M. Gyulassy, P. Levai, and I. Vitev, NonAbelian energy loss at finite opacity, *Phys. Rev. Lett.* **85**, 5535 (2000), [arXiv:nucl-th/0005032](#).
- [8] M. Gyulassy, P. Levai, and I. Vitev, Reaction operator approach to nonAbelian energy loss, *Nucl. Phys. B* **594**, 371 (2001), [arXiv:nucl-th/0006010](#).
- [9] U. A. Wiedemann, Gluon radiation off hard quarks in a nuclear environment: Opacity expansion, *Nucl. Phys. B* **588**, 303 (2000), [arXiv:hep-ph/0005129](#).
- [10] U. A. Wiedemann, Jet quenching versus jet enhancement: A Quantitative study of the BDMPS-Z gluon radiation spectrum, *Nucl. Phys. A* **690**, 731 (2001), [arXiv:hep-ph/0008241](#).
- [11] X.-f. Guo and X.-N. Wang, Multiple scattering, parton energy loss and modified fragmentation functions in deeply inelastic e A scattering, *Phys. Rev. Lett.* **85**, 3591 (2000), [arXiv:hep-ph/0005044](#).
- [12] X.-N. Wang and X.-f. Guo, Multiple parton scattering in nuclei: Parton energy loss, *Nucl. Phys. A* **696**, 788 (2001), [arXiv:hep-ph/0102230](#).
- [13] A. Majumder, Hard collinear gluon radiation and multiple scattering in a medium, *Phys. Rev. D* **85**, 014023 (2012), [arXiv:0912.2987 \[nucl-th\]](#).
- [14] P. B. Arnold, G. D. Moore, and L. G. Yaffe, Photon emission from ultrarelativistic plasmas, *JHEP* **11**, 057, [arXiv:hep-ph/0109064](#).
- [15] P. B. Arnold, G. D. Moore, and L. G. Yaffe, Photon and gluon emission in relativistic plasmas, *JHEP* **06**, 030, [arXiv:hep-ph/0204343](#).
- [16] A. Majumder and M. Van Leeuwen, The Theory and Phenomenology of Perturbative QCD Based Jet Quenching, *Prog. Part. Nucl. Phys.* **66**, 41 (2011), [arXiv:1002.2206 \[hep-ph\]](#).
- [17] J. P. Blaizot and Y. Mehtar-Tani, Jet Structure in Heavy Ion Collisions, *Int. J. Mod. Phys. E* **24**, 1530012 (2015), [arXiv:1503.05958 \[hep-ph\]](#).
- [18] G.-Y. Qin and X.-N. Wang, Jet quenching in high-energy heavy-ion collisions, *Int. J. Mod. Phys. E* **24**, 1530014 (2015), [arXiv:1511.00790 \[hep-ph\]](#).
- [19] S. Cao and X.-N. Wang, Jet quenching and medium response in high-energy heavy-ion collisions: a review, *Rept. Prog. Phys.* **84**, 024301 (2021), [arXiv:2002.04028 \[hep-ph\]](#).
- [20] S. Cao, A. Majumder, R. Modarresi-Yazdi, I. Soudi, and Y. Tachibana, Jet quenching: From theory to simulation, *Int. J. Mod. Phys. E* **33**, 2430002 (2024), [arXiv:2401.10026 \[hep-ph\]](#).
- [21] I. Soudi *et al.* (JETSCAPE), A soft-hard framework with exact four momentum conservation for small systems, (2024), [arXiv:2407.17443 \[hep-ph\]](#).
- [22] K. Adcox *et al.* (PHENIX), Suppression of hadrons with large transverse momentum in central Au+Au collisions at $\sqrt{s_{NN}} = 130$ -GeV, *Phys. Rev. Lett.* **88**, 022301 (2002), [arXiv:nucl-ex/0109003](#).
- [23] S. S. Adler *et al.* (PHENIX), High p_T charged hadron suppression in Au + Au collisions at $\sqrt{s_{NN}} = 200$ GeV, *Phys. Rev. C* **69**, 034910 (2004), [arXiv:nucl-ex/0308006](#).
- [24] S. S. Adler *et al.* (PHENIX), Suppressed π^0 production at large transverse momentum in central Au+ Au collisions at $\sqrt{s_{NN}} = 200$ GeV, *Phys. Rev. Lett.* **91**, 072301 (2003), [arXiv:nucl-ex/0304022](#).
- [25] C. Adler *et al.* (STAR), Centrality dependence of high p_T hadron suppression in Au+Au collisions at $\sqrt{s_{NN}} = 130$ -GeV, *Phys. Rev. Lett.* **89**, 202301 (2002), [arXiv:nucl-ex/0206011](#).
- [26] J. Adams *et al.* (STAR), Transverse momentum and collision energy dependence of high $p(T)$ hadron suppression in Au+Au collisions at ultrarelativistic energies, *Phys. Rev. Lett.* **91**, 172302 (2003), [arXiv:nucl-ex/0305015](#).
- [27] C. Adler *et al.* (STAR), Disappearance of back-to-back high p_T hadron correlations in central Au+Au collisions at $\sqrt{s_{NN}} = 200$ -GeV, *Phys. Rev. Lett.* **90**, 082302 (2003), [arXiv:nucl-ex/0210033](#).
- [28] J. Adams *et al.* (STAR), Distributions of charged hadrons associated with high transverse momentum particles in pp and Au + Au collisions at $s(NN)^{1/2} = 200$ -GeV, *Phys. Rev. Lett.* **95**, 152301 (2005), [arXiv:nucl-ex/0501016](#).
- [29] A. Adare *et al.* (PHENIX), Transverse momentum

- and centrality dependence of dihadron correlations in Au+Au collisions at $s(\text{NN}) = 200\text{-GeV}$: Jet-quenching and the response of partonic matter, *Phys. Rev. C* **77**, 011901 (2008), [arXiv:0705.3238 \[nucl-ex\]](#).
- [30] B. Abelev *et al.* (ALICE), Measurement of charged jet suppression in Pb-Pb collisions at $\sqrt{s_{\text{NN}}} = 2.76\text{ TeV}$, *JHEP* **03**, 013, [arXiv:1311.0633 \[nucl-ex\]](#).
- [31] G. Aad *et al.* (ATLAS), Observation of a Centrality-Dependent Dijet Asymmetry in Lead-Lead Collisions at $\sqrt{s_{\text{NN}}} = 2.77\text{ TeV}$ with the ATLAS Detector at the LHC, *Phys. Rev. Lett.* **105**, 252303 (2010), [arXiv:1011.6182 \[hep-ex\]](#).
- [32] S. Chatrchyan *et al.* (CMS), Observation and studies of jet quenching in PbPb collisions at nucleon-nucleon center-of-mass energy = 2.76 TeV, *Phys. Rev. C* **84**, 024906 (2011), [arXiv:1102.1957 \[nucl-ex\]](#).
- [33] J. Adam *et al.* (STAR), Measurement of inclusive charged-particle jet production in Au + Au collisions at $\sqrt{s_{\text{NN}}} = 200\text{ GeV}$, *Phys. Rev. C* **102**, 054913 (2020), [arXiv:2006.00582 \[nucl-ex\]](#).
- [34] G. Aad *et al.* (ATLAS), Measurement of the jet radius and transverse momentum dependence of inclusive jet suppression in lead-lead collisions at $\sqrt{s_{\text{NN}}} = 2.76\text{ TeV}$ with the ATLAS detector, *Phys. Lett. B* **719**, 220 (2013), [arXiv:1208.1967 \[hep-ex\]](#).
- [35] G. Aad *et al.* (ATLAS), Measurements of the Nuclear Modification Factor for Jets in Pb+Pb Collisions at $\sqrt{s_{\text{NN}}} = 2.76\text{ TeV}$ with the ATLAS Detector, *Phys. Rev. Lett.* **114**, 072302 (2015), [arXiv:1411.2357 \[hep-ex\]](#).
- [36] V. Khachatryan *et al.* (CMS), Measurement of inclusive jet cross sections in *pp* and PbPb collisions at $\sqrt{s_{\text{NN}}} = 2.76\text{ TeV}$, *Phys. Rev. C* **96**, 015202 (2017), [arXiv:1609.05383 \[nucl-ex\]](#).
- [37] L. Adamczyk *et al.* (STAR), Dijet imbalance measurements in *Au + Au* and *pp* collisions at $\sqrt{s_{\text{NN}}} = 200\text{ GeV}$ at STAR, *Phys. Rev. Lett.* **119**, 062301 (2017), [arXiv:1609.03878 \[nucl-ex\]](#).
- [38] M. Aaboud *et al.* (ATLAS), Measurement of the nuclear modification factor for inclusive jets in Pb+Pb collisions at $\sqrt{s_{\text{NN}}} = 5.02\text{ TeV}$ with the ATLAS detector, *Phys. Lett. B* **790**, 108 (2019), [arXiv:1805.05635 \[nucl-ex\]](#).
- [39] S. Acharya *et al.* (ALICE), Measurements of inclusive jet spectra in *pp* and central Pb-Pb collisions at $\sqrt{s_{\text{NN}}} = 5.02\text{ TeV}$, *Phys. Rev. C* **101**, 034911 (2020), [arXiv:1909.09718 \[nucl-ex\]](#).
- [40] A. M. Sirunyan *et al.* (CMS), First measurement of large area jet transverse momentum spectra in heavy-ion collisions, *JHEP* **05**, 284, [arXiv:2102.13080 \[hep-ex\]](#).
- [41] S. Chatrchyan *et al.* (CMS), Modification of Jet Shapes in PbPb Collisions at $\sqrt{s_{\text{NN}}} = 2.76\text{ TeV}$, *Phys. Lett. B* **730**, 243 (2014), [arXiv:1310.0878 \[nucl-ex\]](#).
- [42] V. Khachatryan *et al.* (CMS), Decomposing transverse momentum balance contributions for quenched jets in PbPb collisions at $\sqrt{s_{\text{NN}}} = 2.76\text{ TeV}$, *JHEP* **11**, 055, [arXiv:1609.02466 \[nucl-ex\]](#).
- [43] A. M. Sirunyan *et al.* (CMS), Jet properties in PbPb and *pp* collisions at $\sqrt{s_{\text{NN}}} = 5.02\text{ TeV}$, *JHEP* **05**, 006, [arXiv:1803.00042 \[nucl-ex\]](#).
- [44] A. M. Sirunyan *et al.* (CMS), Jet Shapes of Isolated Photon-Tagged Jets in Pb-Pb and *pp* Collisions at $\sqrt{s_{\text{NN}}} = 5.02\text{ TeV}$, *Phys. Rev. Lett.* **122**, 152001 (2019), [arXiv:1809.08602 \[hep-ex\]](#).
- [45] A. M. Sirunyan *et al.* (CMS), Measurement of the groomed jet mass in PbPb and *pp* collisions at $\sqrt{s_{\text{NN}}} = 5.02\text{ TeV}$, *JHEP* **10**, 161, [arXiv:1805.05145 \[hep-ex\]](#).
- [46] S. Acharya *et al.* (ALICE), Measurement of jet radial profiles in Pb–Pb collisions at $\sqrt{s_{\text{NN}}} = 2.76\text{ TeV}$, *Phys. Lett. B* **796**, 204 (2019), [arXiv:1904.13118 \[nucl-ex\]](#).
- [47] A. M. Sirunyan *et al.* (CMS), In-medium modification of dijets in PbPb collisions at $\sqrt{s_{\text{NN}}} = 5.02\text{ TeV}$, *JHEP* **05**, 116, [arXiv:2101.04720 \[hep-ex\]](#).
- [48] S. Chatrchyan *et al.* (CMS), Measurement of Jet Fragmentation in PbPb and *pp* Collisions at $\sqrt{s_{\text{NN}}} = 2.76\text{ TeV}$, *Phys. Rev. C* **90**, 024908 (2014), [arXiv:1406.0932 \[nucl-ex\]](#).
- [49] G. Aad *et al.* (ATLAS), Measurement of inclusive jet charged-particle fragmentation functions in Pb+Pb collisions at $\sqrt{s_{\text{NN}}} = 2.76\text{ TeV}$ with the ATLAS detector, *Phys. Lett. B* **739**, 320 (2014), [arXiv:1406.2979 \[hep-ex\]](#).
- [50] M. Aaboud *et al.* (ATLAS), Measurement of jet fragmentation in Pb+Pb and *pp* collisions at $\sqrt{s_{\text{NN}}} = 2.76\text{ TeV}$ with the ATLAS detector at the LHC, *Eur. Phys. J. C* **77**, 379 (2017), [arXiv:1702.00674 \[hep-ex\]](#).
- [51] M. Aaboud *et al.* (ATLAS), Measurement of jet fragmentation in Pb+Pb and *pp* collisions at $\sqrt{s_{\text{NN}}} = 5.02\text{ TeV}$ with the ATLAS detector, *Phys. Rev. C* **98**, 024908 (2018), [arXiv:1805.05424 \[nucl-ex\]](#).
- [52] M. Aaboud *et al.* (ATLAS), Comparison of Fragmentation Functions for Jets Dominated by Light Quarks and Gluons from *pp* and Pb+Pb Collisions in ATLAS, *Phys. Rev. Lett.* **123**, 042001 (2019), [arXiv:1902.10007 \[nucl-ex\]](#).
- [53] G. Aad *et al.* (ATLAS), Measurement of angular and momentum distributions of charged particles within and around jets in Pb+Pb and *pp* collisions at $\sqrt{s_{\text{NN}}} = 5.02\text{ TeV}$ with the ATLAS detector, *Phys. Rev. C* **100**, 064901 (2019), [Erratum: *Phys. Rev. C* **101**, 059903 (2020)], [arXiv:1908.05264 \[nucl-ex\]](#).
- [54] L. Apolinário, Y.-T. Chien, and L. Cunqueiro Mendez, Jet substructure, *Int. J. Mod. Phys. E* **33**, 2430003 (2024).
- [55] A. Hayrapetyan *et al.* (CMS), Girth and groomed radius of jets recoiling against isolated photons in lead-lead and proton-proton collisions at $\sqrt{s_{\text{NN}}} = 5.02\text{ TeV}$, *Phys. Lett. B* **861**, 139088 (2025), [arXiv:2405.02737 \[nucl-ex\]](#).
- [56] S. Acharya *et al.* (ALICE), Search for quasi-particle scattering in the quark-gluon plasma with jet splittings in *pp* and Pb–Pb collisions at $\sqrt{s_{\text{NN}}} = 5.02\text{ TeV}$, (2024), [arXiv:2409.12837 \[nucl-ex\]](#).
- [57] S. Acharya *et al.* (ALICE), Medium-induced modification of groomed and ungroomed jet mass and angularities in Pb-Pb collisions at $\sqrt{s_{\text{NN}}} = 5.02\text{ TeV}$, (2024), [arXiv:2411.03106 \[nucl-ex\]](#).
- [58] J. M. Butterworth, A. R. Davison, M. Rubin, and G. P. Salam, Jet substructure as a new Higgs search channel at the LHC, *Phys. Rev. Lett.* **100**, 242001 (2008), [arXiv:0802.2470 \[hep-ph\]](#).
- [59] D. Krohn, J. Thaler, and L.-T. Wang, Jet Trimming, *JHEP* **02**, 084, [arXiv:0912.1342 \[hep-ph\]](#).
- [60] S. D. Ellis, C. K. Vermilion, and J. R. Walsh, Recombination Algorithms and Jet Substructure: Pruning as a Tool for Heavy Particle Searches, *Phys. Rev. D* **81**, 094023 (2010), [arXiv:0912.0033 \[hep-ph\]](#).
- [61] M. Dasgupta, A. Fregoso, S. Marzani, and G. P. Salam, Towards an understanding of jet substructure, *JHEP* **09**, 029, [arXiv:1307.0007 \[hep-ph\]](#).
- [62] A. J. Larkoski, S. Marzani, G. Soyez, and J. Thaler, Soft

- Drop, *JHEP* **05**, 146, [arXiv:1402.2657 \[hep-ph\]](#).
- [63] A. J. Larkoski, S. Marzani, and J. Thaler, Sudakov Safety in Perturbative QCD, *Phys. Rev. D* **91**, 111501 (2015), [arXiv:1502.01719 \[hep-ph\]](#).
- [64] Y. Mehtar-Tani, A. Soto-Ontoso, and K. Tywoniuk, Dynamical grooming of QCD jets, *Phys. Rev. D* **101**, 034004 (2020), [arXiv:1911.00375 \[hep-ph\]](#).
- [65] Y.-T. Chien and I. Vitev, Probing the Hardest Branching within Jets in Heavy-Ion Collisions, *Phys. Rev. Lett.* **119**, 112301 (2017), [arXiv:1608.07283 \[hep-ph\]](#).
- [66] Y. Mehtar-Tani and K. Tywoniuk, Groomed jets in heavy-ion collisions: sensitivity to medium-induced bremsstrahlung, *JHEP* **04**, 125, [arXiv:1610.08930 \[hep-ph\]](#).
- [67] N.-B. Chang, S. Cao, and G.-Y. Qin, Probing medium-induced jet splitting and energy loss in heavy-ion collisions, *Phys. Lett. B* **781**, 423 (2018), [arXiv:1707.03767 \[hep-ph\]](#).
- [68] G. Milhano, U. A. Wiedemann, and K. C. Zapp, Sensitivity of jet substructure to jet-induced medium response, *Phys. Lett. B* **779**, 409 (2018), [arXiv:1707.04142 \[hep-ph\]](#).
- [69] J. Casalderrey-Solana, G. Milhano, D. Pablos, and K. Rajagopal, Modification of Jet Substructure in Heavy Ion Collisions as a Probe of the Resolution Length of Quark-Gluon Plasma, *JHEP* **01**, 044, [arXiv:1907.11248 \[hep-ph\]](#).
- [70] F. Ringer, B.-W. Xiao, and F. Yuan, Can we observe jet P_T -broadening in heavy-ion collisions at the LHC?, *Phys. Lett. B* **808**, 135634 (2020), [arXiv:1907.12541 \[hep-ph\]](#).
- [71] P. Caucal, E. Iancu, and G. Soyez, Deciphering the z_g distribution in ultrarelativistic heavy ion collisions, *JHEP* **10**, 273, [arXiv:1907.04866 \[hep-ph\]](#).
- [72] P. Caucal, A. Soto-Ontoso, and A. Takacs, Dynamical Grooming meets LHC data, *JHEP* **07**, 020, [arXiv:2103.06566 \[hep-ph\]](#).
- [73] P. Caucal, A. Soto-Ontoso, and A. Takacs, Dynamically groomed jet radius in heavy-ion collisions, *Phys. Rev. D* **105**, 114046 (2022), [arXiv:2111.14768 \[hep-ph\]](#).
- [74] Y. Tachibana *et al.* (JETSCAPE), Hard jet substructure in a multistage approach, *Phys. Rev. C* **110**, 044907 (2024), [arXiv:2301.02485 \[hep-ph\]](#).
- [75] L. Cunqueiro, D. Pablos, A. Soto-Ontoso, M. Spousta, A. Takacs, and M. Verweij, Isolating perturbative QCD splittings in heavy-ion collisions, *Phys. Rev. D* **110**, 014015 (2024), [arXiv:2311.07643 \[hep-ph\]](#).
- [76] S. Cao and A. Majumder, Nuclear modification of leading hadrons and jets within a virtuality ordered parton shower, *Phys. Rev. C* **101**, 024903 (2020), [arXiv:1712.10055 \[nucl-th\]](#).
- [77] A. Majumder, Incorporating Space-Time Within Medium-Modified Jet Event Generators, *Phys. Rev. C* **88**, 014909 (2013), [arXiv:1301.5323 \[nucl-th\]](#).
- [78] Y. He, T. Luo, X.-N. Wang, and Y. Zhu, Linear Boltzmann Transport for Jet Propagation in the Quark-Gluon Plasma: Elastic Processes and Medium Recoil, *Phys. Rev. C* **91**, 054908 (2015), [Erratum: *Phys. Rev. C* **97**, 019902 (2018)], [arXiv:1503.03313 \[nucl-th\]](#).
- [79] S. Cao, T. Luo, G.-Y. Qin, and X.-N. Wang, Linearized Boltzmann transport model for jet propagation in the quark-gluon plasma: Heavy quark evolution, *Phys. Rev. C* **94**, 014909 (2016), [arXiv:1605.06447 \[nucl-th\]](#).
- [80] Y. He, S. Cao, W. Chen, T. Luo, L.-G. Pang, and X.-N. Wang, Interplaying mechanisms behind single inclusive jet suppression in heavy-ion collisions, *Phys. Rev. C* **99**, 054911 (2019), [arXiv:1809.02525 \[nucl-th\]](#).
- [81] T. Luo, S. Cao, Y. He, and X.-N. Wang, Multiple jets and γ -jet correlation in high-energy heavy-ion collisions, *Phys. Lett. B* **782**, 707 (2018), [arXiv:1803.06785 \[hep-ph\]](#).
- [82] S. Cao *et al.* (JETSCAPE), Multistage Monte-Carlo simulation of jet modification in a static medium, *Phys. Rev. C* **96**, 024909 (2017), [arXiv:1705.00050 \[nucl-th\]](#).
- [83] J. H. Putschke *et al.*, The JETSCAPE framework, (2019), [arXiv:1903.07706 \[nucl-th\]](#).
- [84] A. Kumar *et al.* (JETSCAPE), JETSCAPE framework: $p + p$ results, *Phys. Rev. C* **102**, 054906 (2020), [arXiv:1910.05481 \[nucl-th\]](#).
- [85] D. Everett *et al.* (JETSCAPE), Phenomenological constraints on the transport properties of QCD matter with data-driven model averaging, *Phys. Rev. Lett.* **126**, 242301 (2021), [arXiv:2010.03928 \[hep-ph\]](#).
- [86] D. Everett *et al.* (JETSCAPE), Multisystem Bayesian constraints on the transport coefficients of QCD matter, *Phys. Rev. C* **103**, 054904 (2021), [arXiv:2011.01430 \[hep-ph\]](#).
- [87] S. Cao *et al.* (JETSCAPE), Determining the jet transport coefficient \hat{q} from inclusive hadron suppression measurements using Bayesian parameter estimation, *Phys. Rev. C* **104**, 024905 (2021), [arXiv:2102.11337 \[nucl-th\]](#).
- [88] D. Everett *et al.* (JETSCAPE), Role of bulk viscosity in deuteron production in ultrarelativistic nuclear collisions, *Phys. Rev. C* **106**, 064901 (2022), [arXiv:2203.08286 \[hep-ph\]](#).
- [89] A. Kumar *et al.* (JETSCAPE), Inclusive jet and hadron suppression in a multistage approach, *Phys. Rev. C* **107**, 034911 (2023), [arXiv:2204.01163 \[hep-ph\]](#).
- [90] W. Fan *et al.* (JETSCAPE), Multiscale evolution of charmed particles in a nuclear medium, *Phys. Rev. C* **107**, 054901 (2023), [arXiv:2208.00983 \[nucl-th\]](#).
- [91] W. Fan *et al.* (JETSCAPE), New metric improving Bayesian calibration of a multistage approach studying hadron and inclusive jet suppression, *Phys. Rev. C* **109**, 064903 (2024), [arXiv:2307.09641 \[hep-ph\]](#).
- [92] R. Ehlers *et al.* (JETSCAPE), Bayesian Inference analysis of jet quenching using inclusive jet and hadron suppression measurements, (2024), [arXiv:2408.08247 \[hep-ph\]](#).
- [93] C. Sirimanna *et al.* (JETSCAPE), Hard Photon Triggered Jets in p - p and A - A Collisions, (2024), [arXiv:2412.19738 \[hep-ph\]](#).
- [94] A. Kumar, A. Majumder, and C. Shen, Energy and scale dependence of \hat{q} and the “JET puzzle”, *Phys. Rev. C* **101**, 034908 (2020), [arXiv:1909.03178 \[nucl-th\]](#).
- [95] A. Kumar, A. Majumder, C. Sirimanna, and Y. Tachibana, Modified Coherence and the Transverse Extent of Jets, (2025), [arXiv:2501.07823 \[hep-ph\]](#).
- [96] J. Liu, C. Shen, and U. Heinz, Pre-equilibrium evolution effects on heavy-ion collision observables, *Phys. Rev. C* **91**, 064906 (2015), [Erratum: *Phys. Rev. C* **92**, 049904 (2015)], [arXiv:1504.02160 \[nucl-th\]](#).
- [97] C. Shen, Z. Qiu, H. Song, J. Bernhard, S. Bass, and U. Heinz, The iEBE-VISHNU code package for relativistic heavy-ion collisions, *Comput. Phys. Commun.* **199**, 61 (2016), [arXiv:1409.8164 \[nucl-th\]](#).
- [98] S. A. Bass *et al.*, Microscopic models for ultrarelativistic

- heavy ion collisions, *Prog. Part. Nucl. Phys.* **41**, 255 (1998), [arXiv:nucl-th/9803035](#).
- [99] M. Bleicher *et al.*, Relativistic hadron hadron collisions in the ultrarelativistic quantum molecular dynamics model, *J. Phys. G* **25**, 1859 (1999), [arXiv:hep-ph/9909407](#).
- [100] J. S. Moreland, J. E. Bernhard, and S. A. Bass, Alternative ansatz to wounded nucleon and binary collision scaling in high-energy nuclear collisions, *Phys. Rev. C* **92**, 011901 (2015), [arXiv:1412.4708 \[nucl-th\]](#).
- [101] J. E. Bernhard, J. S. Moreland, and S. A. Bass, Bayesian estimation of the specific shear and bulk viscosity of quark-gluon plasma, *Nature Phys.* **15**, 1113 (2019).
- [102] X.-N. Wang and Y. Zhu, Medium Modification of γ -jets in High-energy Heavy-ion Collisions, *Phys. Rev. Lett.* **111**, 062301 (2013), [arXiv:1302.5874 \[hep-ph\]](#).
- [103] T. Luo, Y. He, S. Cao, and X.-N. Wang, Linear Boltzmann transport for jet propagation in the quark-gluon plasma: Inelastic processes and jet modification, *Phys. Rev. C* **109**, 034919 (2024), [arXiv:2306.13742 \[nucl-th\]](#).
- [104] J. Casalderrey-Solana, E. V. Shuryak, and D. Teaney, Conical flow induced by quenched QCD jets, *J. Phys. Conf. Ser.* **27**, 22 (2005), [arXiv:hep-ph/0411315](#).
- [105] H. Stoecker, Collective flow signals the quark gluon plasma, *Nucl. Phys. A* **750**, 121 (2005), [arXiv:nucl-th/0406018](#).
- [106] Y. Tachibana, Medium response to jet-induced excitation: theory overview, *Nucl. Phys. A* **982**, 156 (2019).
- [107] S. Schlichting and I. Soudi, Medium-induced fragmentation and equilibration of highly energetic partons, *JHEP* **07**, 077, [arXiv:2008.04928 \[hep-ph\]](#).
- [108] T. Luo, Medium response in jet quenching, *Nucl. Phys. A* **1005**, 121992 (2021).
- [109] Y. Mehtar-Tani, S. Schlichting, and I. Soudi, Jet thermalization in QCD kinetic theory, *JHEP* **05**, 91, [arXiv:2209.10569 \[hep-ph\]](#).
- [110] A. K. Chaudhuri and U. Heinz, Effect of jet quenching on the hydrodynamical evolution of QGP, *Phys. Rev. Lett.* **97**, 062301 (2006), [arXiv:nucl-th/0503028](#).
- [111] T. Renk and J. Ruppert, Mach cones in an evolving medium, *Phys. Rev. C* **73**, 011901 (2006), [arXiv:hep-ph/0509036](#).
- [112] L. M. Satarov, H. Stoecker, and I. N. Mishustin, Mach shocks induced by partonic jets in expanding quark-gluon plasma, *Phys. Lett. B* **627**, 64 (2005), [arXiv:hep-ph/0505245](#).
- [113] R. B. Neufeld, B. Muller, and J. Ruppert, Sonic Mach Cones Induced by Fast Partons in a Perturbative Quark-Gluon Plasma, *Phys. Rev. C* **78**, 041901 (2008), [arXiv:0802.2254 \[hep-ph\]](#).
- [114] J. Noronha, M. Gyulassy, and G. Torrieri, Di-Jet Conical Correlations Associated with Heavy Quark Jets in anti-de Sitter Space/Conformal Field Theory Correspondence, *Phys. Rev. Lett.* **102**, 102301 (2009), [arXiv:0807.1038 \[hep-ph\]](#).
- [115] G. Y. Qin, A. Majumder, H. Song, and U. Heinz, Energy and momentum deposited into a QCD medium by a jet shower, *Phys. Rev. Lett.* **103**, 152303 (2009), [arXiv:0903.2255 \[nucl-th\]](#).
- [116] B. Betz, J. Noronha, G. Torrieri, M. Gyulassy, and D. H. Rischke, Universal Flow-Driven Conical Emission in Ultrarelativistic Heavy-Ion Collisions, *Phys. Rev. Lett.* **105**, 222301 (2010), [arXiv:1005.5461 \[nucl-th\]](#).
- [117] R. B. Neufeld and I. Vitev, Parton showers as sources of energy-momentum deposition in the QGP and their implication for shockwave formation at RHIC and at the LHC, *Phys. Rev. C* **86**, 024905 (2012), [arXiv:1105.2067 \[hep-ph\]](#).
- [118] M. Schulc and B. Tomášik, Anisotropic flow of the fireball fed by hard partons, *Phys. Rev. C* **90**, 064910 (2014), [arXiv:1409.6116 \[nucl-th\]](#).
- [119] Y. Tachibana and T. Hirano, Momentum transport away from a jet in an expanding nuclear medium, *Phys. Rev. C* **90**, 021902 (2014), [arXiv:1402.6469 \[nucl-th\]](#).
- [120] Y. Tachibana and T. Hirano, Interplay between Mach cone and radial expansion and its signal in γ -jet events, *Phys. Rev. C* **93**, 054907 (2016), [arXiv:1510.06966 \[nucl-th\]](#).
- [121] Y. Tachibana, N.-B. Chang, and G.-Y. Qin, Full jet in quark-gluon plasma with hydrodynamic medium response, *Phys. Rev. C* **95**, 044909 (2017), [arXiv:1701.07951 \[nucl-th\]](#).
- [122] M. Okai, K. Kawaguchi, Y. Tachibana, and T. Hirano, New approach to initializing hydrodynamic fields and mini-jet propagation in quark-gluon fluids, *Phys. Rev. C* **95**, 054914 (2017), [arXiv:1702.07541 \[nucl-th\]](#).
- [123] W. Chen, S. Cao, T. Luo, L.-G. Pang, and X.-N. Wang, Effects of jet-induced medium excitation in γ -hadron correlation in A+A collisions, *Phys. Lett. B* **777**, 86 (2018), [arXiv:1704.03648 \[nucl-th\]](#).
- [124] N.-B. Chang, Y. Tachibana, and G.-Y. Qin, Nuclear modification of jet shape for inclusive jets and γ -jets at the LHC energies, *Phys. Lett. B* **801**, 135181 (2020), [arXiv:1906.09562 \[nucl-th\]](#).
- [125] Y. Tachibana, C. Shen, and A. Majumder, Bulk medium evolution has considerable effects on jet observables, *Phys. Rev. C* **106**, L021902 (2022), [arXiv:2001.08321 \[nucl-th\]](#).
- [126] Y. Tachibana *et al.* (JETSCAPE), Hydrodynamic response to jets with a source based on causal diffusion, *Nucl. Phys. A* **1005**, 121920 (2021), [arXiv:2002.12250 \[nucl-th\]](#).
- [127] J. Casalderrey-Solana, J. G. Milhano, D. Pablos, K. Rajagopal, and X. Yao, Jet Wake from Linearized Hydrodynamics, *JHEP* **05**, 230, [arXiv:2010.01140 \[hep-ph\]](#).
- [128] Z. Yang, W. Chen, Y. He, W. Ke, L. Pang, and X.-N. Wang, Search for the Elusive Jet-Induced Diffusion Wake in Z/γ -Jets with 2D Jet Tomography in High-Energy Heavy-Ion Collisions, *Phys. Rev. Lett.* **127**, 082301 (2021), [arXiv:2101.05422 \[hep-ph\]](#).
- [129] Z. Yang, T. Luo, W. Chen, L.-G. Pang, and X.-N. Wang, 3D Structure of Jet-Induced Diffusion Wake in an Expanding Quark-Gluon Plasma, *Phys. Rev. Lett.* **130**, 052301 (2023), [arXiv:2203.03683 \[hep-ph\]](#).
- [130] D. Pablos, M. Singh, S. Jeon, and C. Gale, Minijet quenching in a concurrent jet+hydro evolution and the nonequilibrium quark-gluon plasma, *Phys. Rev. C* **106**, 034901 (2022), [arXiv:2202.03414 \[nucl-th\]](#).
- [131] Z. Yang, Y. He, W. Chen, W.-Y. Ke, L.-G. Pang, and X.-N. Wang, Deep learning assisted jet tomography for the study of Mach cones in QGP, *Eur. Phys. J. C* **83**, 652 (2023), [arXiv:2206.02393 \[nucl-th\]](#).
- [132] T. Sjöstrand, The PYTHIA Event Generator: Past, Present and Future, *Comput. Phys. Commun.* **246**, 106910 (2020), [arXiv:1907.09874 \[hep-ph\]](#).
- [133] Y. L. Dokshitzer, G. D. Leder, S. Moretti, and B. R. Webber, Better jet clustering algorithms, *JHEP* **08**, 001, [arXiv:hep-ph/9707323](#).

- [134] M. Wobisch and T. Wengler, Hadronization corrections to jet cross-sections in deep inelastic scattering, in *Workshop on Monte Carlo Generators for HERA Physics (Plenary Starting Meeting)* (1998) pp. 270–279, [arXiv:hep-ph/9907280](#).
- [135] M. Cacciari, G. P. Salam, and G. Soyez, The anti- k_t jet clustering algorithm, *JHEP* **04**, 063, [arXiv:0802.1189 \[hep-ph\]](#).
- [136] M. Cacciari and G. P. Salam, Dispelling the N^3 myth for the k_t jet-finder, *Phys. Lett. B* **641**, 57 (2006), [arXiv:hep-ph/0512210](#).
- [137] M. Cacciari, G. P. Salam, and G. Soyez, FastJet User Manual, *Eur. Phys. J. C* **72**, 1896 (2012), [arXiv:1111.6097 \[hep-ph\]](#).
- [138] <https://fastjet.hepforge.org/contrib/>.
- [139] S. Acharya *et al.* (A Large Ion Collider Experiment, ALICE), Measurement of the groomed jet radius and momentum splitting fraction in pp and Pb–Pb collisions at $\sqrt{s_{NN}} = 5.02$ TeV, *Phys. Rev. Lett.* **128**, 102001 (2022), [arXiv:2107.12984 \[nucl-ex\]](#).
- [140] G. Aad *et al.* (ATLAS), Measurement of substructure-dependent jet suppression in Pb+Pb collisions at 5.02 TeV with the ATLAS detector, *Phys. Rev. C* **107**, 054909 (2023), [arXiv:2211.11470 \[nucl-ex\]](#).
- [141] R. Ehlers (ALICE), Exploring medium properties with hard transverse momentum splittings using groomed jet substructure measurements in Pb-Pb collisions with ALICE, *PoS HardProbes2023*, 136 (2024), [arXiv:2310.07065 \[nucl-ex\]](#).
- [142] R. Pordes *et al.*, The Open Science Grid, *J. Phys. Conf. Ser.* **78**, 012057 (2007).
- [143] I. Sfiligoi, D. C. Bradley, B. Holzman, P. Mhashilkar, S. Padhi, and F. Wurthwein, The pilot way to Grid resources using glideinWMS, *WRI World Congress* **2**, 428 (2009).